Inverse modeling of large-scale spatially distributed vadose zone properties using global optimization

Jasper A. Vrugt

Institute for Biodiversity and Ecosystem Dynamics, Faculty of Science, University of Amsterdam, Amsterdam, Netherlands

Gerrit Schoups, Jan W. Hopmans, Chuck Young, Wesley W. Wallender, and Thomas Harter

Hydrology Program, Department of Land, Air and Water Resources, University of California, Davis, California, USA

Willem Bouten

Institute for Biodiversity and Ecosystem Dynamics, Faculty of Science, University of Amsterdam, Amsterdam, Netherlands

Received 25 September 2003; revised 23 February 2004; accepted 29 March 2004; published 15 June 2004.

[1] Computational capabilities have evolved to a point where it is possible to use multidimensional physically based hydrologic models to study spatial and temporal patterns of water flow in the vadose zone. However, models based on multidimensional governing equations have only received limited attention, in particular because of their computational, distributed input, and parameter estimation requirements. The aim of the present paper is to explore the usefulness and applicability of the inverse method to estimate vadose zone properties using the solution of a physically based, distributed three-dimensional model combined with spatially distributed measured tile drainage data from the 3880-ha Broadview Water District (BWD) in the San Joaquin Valley of California. The inverse problem is posed within a single-criterion Bayesian framework and solved by means of the computerized Shuffled Complex Evolution Metropolis global optimization algorithm. To study the benefits of using a spatially distributed three-dimensional vadose zone model, the results of the 3-D model were compared with those obtained using a simple storage-based bucket model and a spatially averaged one-dimensional unsaturated water flow model for a 2-year period. District-wide results demonstrate that measured spatially distributed patterns of drainage data contain only limited information for the identification of vadose zone model parameters and are particularly inadequate to identify the soil hydraulic properties. In contrast, the drain conductance and a soil matrix bypass coefficient were well determined, indicating that the dominant hydrology of the BWD was determined by drain system properties and preferential flow. Despite the significant CPU time needed for model calibration, results suggest that there are advantages in using physically based hydrologic models to study spatial and temporal patterns of water flow at the scale of a watershed. These models not only generate consistent forecasts of spatially distributed drainage data during the calibration and validation period but also possess unbiased predictive capabilities with respect to measured groundwater table depths not included in the calibration. *INDEX TERMS:* 1836 Hydrology: Hydrologic budget (1655); 1842 Hydrology: Irrigation; 1866 Hydrology: Soil moisture; 1871 Hydrology: Surface water quality; 1894 Hydrology: Instruments and techniques; *KEYWORDS:* drainage, unsaturated water flow, soil hydraulic properties, parameter estimation, preferential flow, parameter uncertainty

Citation: Vrugt, J. A., G. Schoups, J. W. Hopmans, C. Young, W. W. Wallender, T. Harter, and W. Bouten (2004), Inverse modeling of large-scale spatially distributed vadose zone properties using global optimization, *Water Resour. Res.*, *40*, W06503, doi:10.1029/2003WR002706.

1. Introduction and Scope

[2] The predictive capability of unsaturated flow and transport models relies heavily on accurate estimates of the soil water retention and unsaturated soil hydraulic characteristics at the application scale of the model. To enable such accurate soil physical characterization, methodologies need to be developed that allow a rapid, reliable, and cost-effective estimation of the hydraulic properties of the considered soil domain, including its spatial variability. Most of the early work reporting on the estimation of hydraulic properties of unsaturated soils has focused on relatively small soil samples using static or steady state flow experiments. These static or steady state flow experiments have the advantage of being relatively simple to implement.

0043-1397/04/2003WR002706$09.00

However, these methods are typically time consuming and require restrictive initial and boundary conditions to satisfy the assumptions of the corresponding analytical solutions.

[3] Significant advances in computational capabilities have resulted in Inverse Modeling (IM) applications for the estimation of soil hydraulic properties from small soil cores [*Durner et al.*, 1997; *Hopmans et al.*, 2002a]. However, when using an IM approach, the soil hydraulic properties can no longer be estimated by direct inversion but are determined using an iterative solution, thereby placing a heavy demand on computational resources. In this iterative process, the soil water retention and unsaturated soil hydraulic conductivity characteristics are indirectly determined from repeated numerical simulations of the governing Richards' equation:

$$C(h_m)\frac{\partial h_m}{\partial t} = \nabla \cdot [\boldsymbol{K}(h_m)\nabla(h_m + z)] + A(x, y, z, t) \qquad (1)$$

thereby minimizing the difference between the observed and model predicted flow variables such as water content and fluxes. Using one-, two-, or three-dimensional forms, this transient equation solves for soil water matric potential, water content and water flux density as a function of time and space. In equation (1), C denotes the soil water capacity (L^{-1}), K is the unsaturated hydraulic conductivity tensor (L T^{-1}), h_m is the soil water matric head (L), z (L) denotes the gravitational head to be included for the vertical flow component only, and A (L^3 L^{-3} T^{-1}) is the volumetric sink term, representing sources and/or sinks of water. For isotropic soils, K simplifies to a scalar that is a function of both h_m and the spatial coordinates. Boundary conditions must be included to allow for specified soil water potentials or fluxes at all boundaries of the simulated unsaturated soil domain. Moreover, user-specified initial conditions and time-varying source/sink terms need be specified. Both, the soil water retention and unsaturated hydraulic conductivity functions (referred to as soil hydraulic functions) are highly nonlinear, with h_m and K varying many orders of magnitude over the water content range that significantly contributes to water flow.

[4] Research on the applicability and suitability of the inverse approach toward identification of the soil hydraulic properties has focused primarily on five issues, (1) the type of transient experiment and kind of prescribed initial and boundary conditions suited to yield a reliable characterization of the soil hydraulic properties [*Hopmans et al.*, 2002a; *van Dam et al.*, 1992, 1994; *Ciollaro and Romano*, 1995; *Santini et al.*, 1995; *Šimůnek and van Genuchten*, 1996, 1997; *Šimůnek et al.*, 1998a; *Romano and Santini*, 1999; *Durner et al.*, 1997; *Wildenschild et al.*, 2001], (2) the determination of the appropriate quantity and most informative kind of observational data [e.g., *Zachmann et al.*, 1981; *Kool et al.*, 1985; *Parker et al.*, 1985; *Kool and Parker*, 1988; *Valiantzas and Kerkides*, 1990; *Toorman et al.*, 1992; *Eching and Hopmans*, 1993; *Eching et al.*, 1994], (3) the selection of an appropriate model of the soil hydraulic properties [*Zachmann et al.*, 1982; *Russo*, 1988; *Zurmühl and Durner*, 1998], (4) the construction and weighting of multiple sources of information in an objective function [*van Dam et al.*, 1994; *Hollenbeck and Jensen*, 1998; *Vrugt and Bouten*, 2002], and (5) the adoption and development of Bayesian and multiple-criteria parameter estimation strategies that can be used to quantify the uncertainty (probabilistic and multiobjective) associated with the inversely estimated soil hydraulic properties [*Kool and Parker*, 1988; *Hollenbeck and Jensen*, 1998; *Vrugt and Bouten*, 2002; *Vrugt et al.*, 2003a]. With these developments, the capabilities and limitations of the inverse approach for the identification of soil hydraulic properties from laboratory soil cores may be considered reasonably well understood. Despite this progress made, still little is known about the suitability of the inverse approach for the identification of vadose zone properties at larger spatial scales.

[5] It has been a major challenge to integrate these small-scale measurements of soil hydraulic properties in hydrologic models that apply across a range of spatial and temporal scales [*Gelhar*, 1986; *Grayson and Blöschl*, 2001]. In most applications, prediction of soil-water dynamics at larger spatial scales uses soil hydraulic properties determined from laboratory core or small field plot measurements, and are included in hydrologic models with a grid or element size much larger than the core or field plot scale. Because of the high nonlinearity of the soil hydraulic functions, their application across spatial scales is inherently problematic. Specifically, the averaging of processes determined from discrete small-scale samples may not be representative of the key hydrologic processes of the larger spatial domain. In addition, the dominant hydrologic flow processes may vary between spatial scales, so that potentially different models need to be used to describe water flow at the soil pedon, field, or watershed scale.

[6] Typically, in hydrologic studies of large spatial dimensions, one may apply a deterministic approach, using a distributed physically based model with upscaled effective soil properties [*Blöschl et al.*, 1995] or use stochastic modeling. A stochastic model preserves the small-scale characteristics of the measurement, but provides estimates of effective properties at the larger spatial scale after accounting for spatial heterogeneity of hydraulic properties. Stochastic approaches to upscale soil hydrologic processes from the local to the field scale include analytical models, based primarily on perturbation approximations of Richards' equation [e.g., *Zhang*, 2002]. Alternatively, numerical stochastic models have used Monte Carlo (MC) simulations to derive effective field-scale hydraulic properties and to predict field-scale hydraulic behavior based on local-scale measurements [*Hopmans and Stricker*, 1989; *Harter and Yeh*, 1998; *Harter and Zhang*, 1999]. Any of these approaches can become computationally intensive, requiring a large number of model simulations.

[7] Instead of a formal upscaling technique that incorporates nonlinear effects on upscaled soil properties applicable across a range of spatial domains, we here propose using a deterministic inverse modeling approach [*Hopmans et al.*, 2002b]. To estimate effective vadose zone parameters, a parameter optimization technique will be applied that is consistent regarding the spatial and temporal scale of the measurement and model parameter support. However, unlike in small-scale experiments, boundary and initial conditions at the larger spatial scales are not as clearly defined because direct measurement techniques are mostly not available. Furthermore, the data available to characterize large-scale vadose processes are sparse, both in space and

time. Both these factors lead to significant uncertainty when estimating effective large-scale parameters. Therefore the application of deterministic inverse modeling at the watershed scale must account for the uncertainty of the estimated large-scale parameters and the associated prediction uncertainty. This requires the use of statistically based parameter estimation algorithms. An additional key element of the proposed distributed approach is that the applied vadose zone model must be able to simulate the key hydrologic processes that dominate the larger spatial domain, by using appropriate effective hydrologic parameters. This requires the use of a process-based model that incorporates functional distributed vadose zone parameters that can account for the relevant observed hydrologic processes.

[8] Current computational capabilities have evolved to a point, where it is now possible to use multidimensional physically based watershed models to study spatial and temporal patterns of water flow in the vadose zone [*Beven*, 2001; *Madsen*, 2003; *Panday and Huyakorn*, 2004]. With the availability of powerful personal computers, efficient computational methods, and sophisticated GIS, remote sensing and advanced visualizations tools, the hydrologic community is beginning to take advantage of the potential and utility of these physically based numerical models. With few exceptions, these models are based on complex multi-dimensional governing equations. They have received limited attention, primarily because of their computational, distributed input, and parameter estimation requirements.

[9] Considerable progress has been made in the application of automated optimization algorithms to estimate hydrologic model parameters across a range of spatial scales. However, emphasis is mostly placed on the estimation of a single optimal set of model parameters, thereby effectively neglecting the influence of parameter uncertainty. Such uncertainties arise mainly from the inability of the calibration process to uniquely identify a single optimal parameter set, from measurement errors associated with system input and output and from model structure errors. The hydrologic community is increasingly aware that hydrologic model identification and evaluation procedures should explicitly include uncertainty estimates [*Kuczera and Parent*, 1998; *Bates and Campbell*, 2001; *Thyer et al.*, 2002; *Vrugt et al.*, 2003a, 2003b, 2003c, 2004]. To acknowledge the presence of parameter uncertainty and to develop a tool that can be used to estimate this uncertainty, *Vrugt et al.* [2003b], recently developed the Shuffled Complex Evolution Metropolis-University of Amsterdam/Arizona (SCEM-UA) global optimization algorithm. The SCEM-UA algorithm is a general purpose global optimization algorithm that provides an efficient estimate of the most likely parameter set and its underlying posterior probability distribution within a single optimization run. The algorithm is an extension of the SCE-UA population evolution method developed by *Duan et al.* [1992].

[10] The aim of the present paper is to explore the usefulness and applicability of this inverse method to estimate vadose zone parameters at the small catchment and watershed scale by using spatially distributed tile drainage data as calibration targets. We hypothesize that the proposed inverse modeling approach will significantly improve our understanding of unsaturated water flow at larger spatial and temporal scales. To test the proposed model calibration approach, we selected the 3880-ha Broadview Water District (BWD), located on the west side of the San Joaquin Valley of California. The BWD has been the subject of various investigations [*Vaughan and Corwin*, 1994; *Vaughan et al.*, 1995, 1999; *Bourgault et al.*, 1997; *Corwin et al.*, 1999]. These research efforts have resulted in a comprehensive measurement data set of spatially distributed, weekly tile drainage flows and groundwater table depths throughout the district. This data set provides a unique opportunity to study spatial and temporal patterns of soil water flow by inverse modeling. As in other watersheds, however, this data set includes considerable uncertainties, arising from unknown soil properties, limited information about the spatial variations in rainfall, crop transpiration and soil evaporation across BWD, and the unknown spatial distribution of groundwater flow. In this paper, we compare three different mathematical models (representing different levels of model complexity) and consider three spatial resolution scales (field, drainage unit, and water district scale) for their ability to minimize uncertainty in the calibration parameters while also minimizing model prediction errors.

[11] The remainder of this paper is organized by sections. Section 2 discusses the BWD including an overview of the measurements that are available for model calibration, presents a condensed description of the MODHMS and BUCKET hydrologic models, and describes the SCEM-UA algorithm, which is used to solve for the single criterion optimization problem. In section 3, we explore the usefulness and applicability of the combined MODHMS-inverse methodology for the identification of vadose zone properties across a range of spatial scales using varying model complexity and spatial resolution of the boundary conditions. Fully integrated three-dimensional solutions of the Richards' equation (1) with spatially distributed boundary conditions are compared with results from a simplified conceptual bucket model and with one-dimensional solutions of the unsaturated flow equation with upscaled, spatially averaged boundary conditions. Finally, a summary with conclusions is presented in section 4.

2. Materials and Methods

2.1. Field Site

[12] The 3880-ha (9700 acres) Broadview Water District (BWD) is part of the San Joaquin Valley watershed and is located approximately 100 km west of Fresno (Figure 1). The district meets several criteria that are intrinsically important to the objectives of this study: (1) The district's size is typical for midsized watersheds, much larger than the typical field scale. (2) An extensive tile-drain system underlies much of the district, which creates tight coupling between vadose zone, shallow groundwater, and drainage fluxes. (3) A comprehensive data set of measured input and output data is available, which relates the measured surface boundary conditions to spatial drainage patterns, measured in sumps of 25 tile-drained drain units, and groundwater table depths.

[13] The western San Joaquin Valley is topographically flat with southwest-northeast sloping deposits with slopes less than 1%. The geomorphic landscape consists of a series

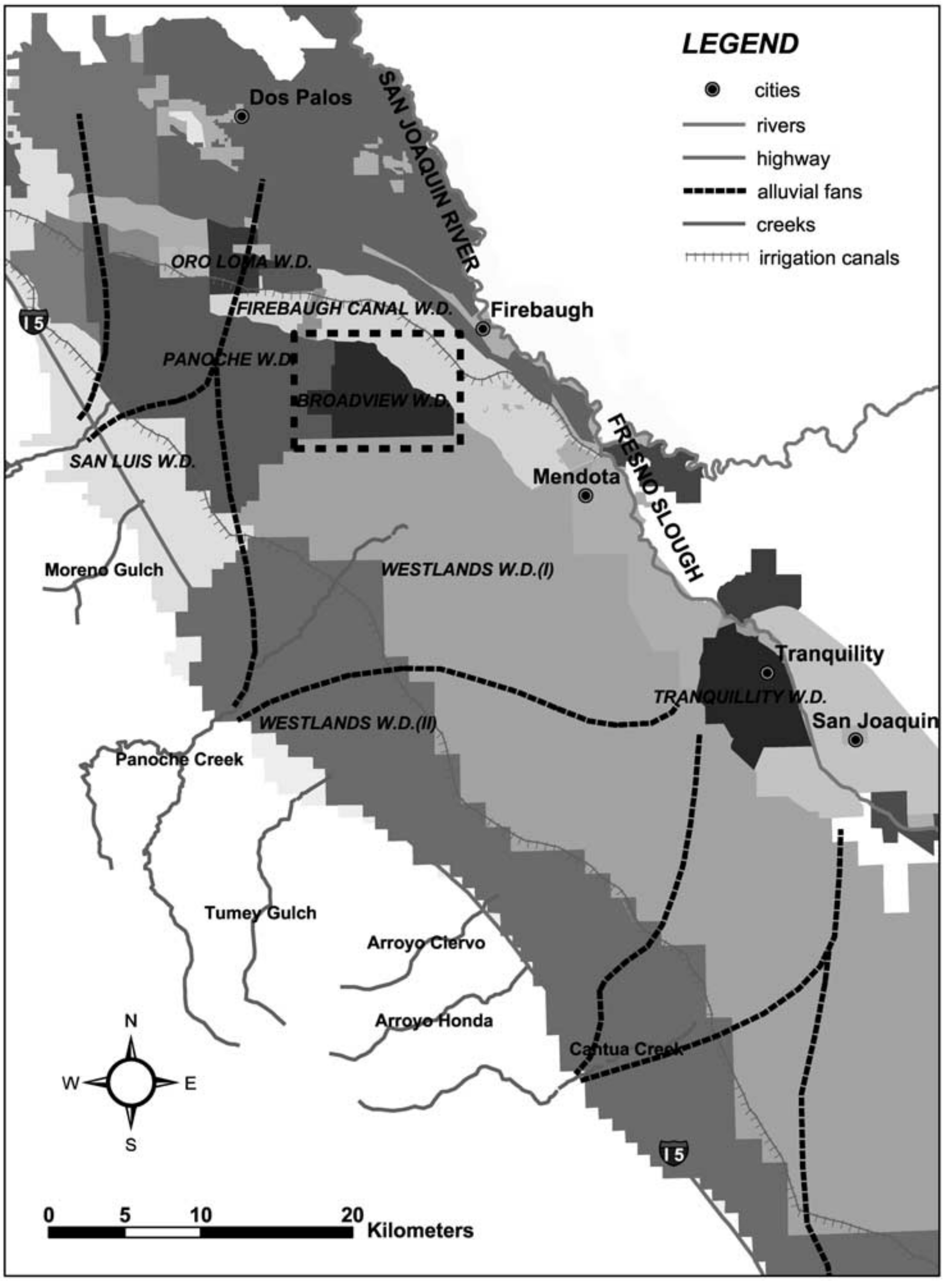

Figure 1. Site map: location of the Broadview Water District (BWD) in the San Joaquin Valley of California.

of alluvial fans that have been deposited by intermittent streams originating in the Coast Ranges to the west. The BWD is located on the Panoche Creek alluvial fan (Figure 1). These alluvial deposits are derived from marine sedimentary calcareous and gypsiferous shales and sandstones of the Coast Ranges [*Harradine*, 1950]. They are underlain by the Corcoran clay, a lacustrine clay deposit that extends throughout the region, and lies at depths of 244 m (valley margin) to 30 m (near river) below the surface [*Belitz*, 1988]. The alluvial soils derived from the Coast Range alluvium are generally fine-textured soils, with an average clay content of 50%. The clay fraction is dominated by montmorillonite, with significant swelling and shrinking properties, accounting for most of the cation exchange behavior. Organic matter contents are less than 1%. Most soils are calcareous and gypsiferous.

2.1.1. Field Description

[14] Figure 2 presents a schematic overview of the BWD. Most of the water district is divided into quarter sections, each with an approximate area of 64 ha (160 acres). Some smaller fields exist near the district boundary that have irregular shapes. The total district consists of about 60 tile-drained 64-ha agricultural fields. Tile drains are installed at depths of 1.6 to 2 m. Horizontal drain spacings range from 100 m to 200 m. Sumps are located in the northeast corner of each of the drainage units for collection and disposal of drainage water. The eight fields shown in white (numbered "26"), are without a tile-drain system. We assumed that

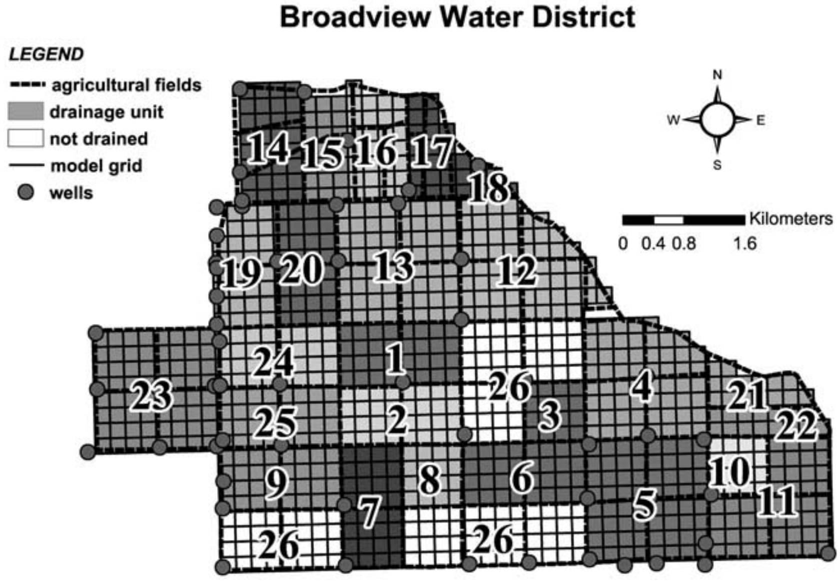

Figure 2. Schematic overview of the BWD. The numbers refer to individual drainage units, which may consist of a single field, two adjacent fields, or all four agricultural fields in a 1.6 km by 1.6 km (1 mile^2) land section.

their irrigation would not affect the water balance of the surrounding fields or drainage units, and were not included in our analysis. Table 1 lists the cropping areas for 1995 and 1996. The main crops are cotton, tomatoes, alfalfa, melons, and wheat.

2.1.2. Measurements

[15] The district maintains irrigation turnouts in the southwest corner of each field. Fields are either furrow or sprinkler irrigated. Water supplied from these irrigation turnouts (I) was measured every 2 days (bi-daily) with an approximate precision of about 120 m^3 (0.1 acre-feet). The cumulative drainage water from each drainage unit, Q_{drain}, was measured weekly at 25 sumps. Water draining into the sumps is pumped into drainage ditches and metered to the same precision as the irrigation water. Additionally, groundwater table measurements were measured in various wells (see Figure 2) at irregular time intervals. A detailed description of the measurements in the BWD is presented by *Vaughan et al.* [1999].

[16] Weekly rainfall amounts and reference evapotranspiration ET_0 were provided by the Firebaugh weather station of the California Irrigation Management Information System (CIMIS). Evapotranspiration was estimated by two separate procedures for the growing and for the fallow seasons. For the growing season, field-specific actual crop evapotranspiration values (ET_c) were estimated using the standard crop coefficient approach [*Allen et al.*, 1998]:

$$ET_c = K_c ET_0 \tag{2}$$

where K_c is the crop coefficient and ET_0 is reference evapotranspiration for grass. Local information on time-varying crop coefficients and crop-specific planting dates were taken from *Snyder et al.* [1989]. Actual evapotranspiration rates were distributed over the root zone assuming a trapezoidal root distribution function. A piecewise linear crop water stress function [*Feddes et al.*, 1978] was used that reduces crop transpiration if the soil water pressure falls below −3 m. Typical parameter values for various crops were taken from *van Dam et al.* [1997].

[17] Soil evaporation during the fallow season, E_s, was estimated external to the models described below using a one-dimensional unsaturated flow model (HYDRUS-1D [*Šimůnek et al.*, 1998b]) that solves equation (1) subject to measured daily rainfall events and daily potential evapotranspiration rates as the upper boundary condition and a constant water table at 2 m as lower boundary condition. Soil hydraulic properties were set identical to those for the MODHMS simulations (see below).

[18] These upper boundary fluxes were computed at the field scale. In some of the case studies, we used upscaled

Table 1. Cropping Areas for the Broadview Water District for 1995 and 1996

Crop	Ha
1995	
Alfalfa seed	348.8
Cotton	1972.5
Fallow	184.1
Garbanzo beans	54.6
Melons	284.5
Oats and melons	22.3
Tomatoes	806.1
Vetch oats	20.2
Total	3648.2
1996	
Alfalfa seed	356.1
Barley and melons	8.1
Cotton	2370.2
Fallow	27.5
Melons	364.2
Tomatoes	461.3
Wheat	60.7
Total	3648.2

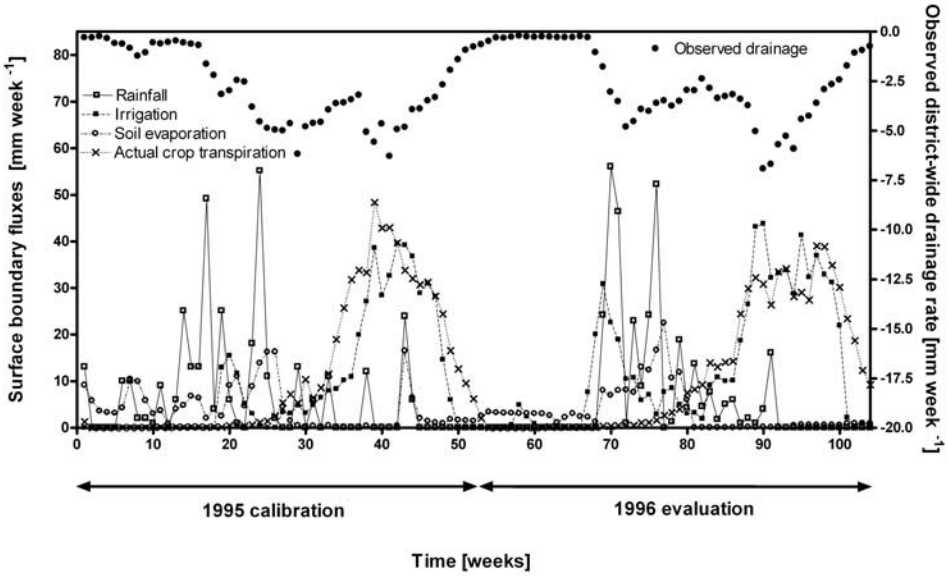

Figure 3. Weekly calculated soil surface boundary conditions for 1995 and 1996 (time 0 corresponds to 1 October 1994). Also included is the spatially averaged weekly measured drainage data of the BWD.

boundary fluxes at the individual drainage unit scale and at the BWD scale. These were computed as area-weighted averages of the individual field-scale fluxes: irrigation, I, precipitation, P, actual crop transpiration, ET_c, and soil evaporation, E_s (all expressed in units of (L T^{-1})). Average depth to groundwater within each drainage unit was estimated by averaging of the available local groundwater table measurements (Figure 2). Figure 3 shows average weekly boundary fluxes and drainage flow (mm week^{-1}) at the BWD scale for the 1995 and 1996 water years (1 October 1994 through 30 September 1996). Because of poor data quality, drainage unit 5 was not further used throughout the remainder of this study, thereby reducing the number of drainage units to 24.

[19] While the measurement data set, by all practical standards, is exceptionally rich in its spatiotemporal resolution, it does not account for actual irrigation and crop water uptake nonuniformity or soil variability at the subfield scale, uncertainty in irrigation application timing between various subsections of individual fields, and nonuniformity of precipitation and ET_0 at the subdistrict scale. A key objective of this paper is to determine whether such a data set contains sufficient information to accurately identify the vadose zone model parameters, despite potentially measurement and boundary condition errors.

2.2. Hydrologic Models

[20] In the past 3 decades, there has been an evolution in hydrologic watershed models for simulation of both single-event and continuous hydrologic processes. Earlier models quantified various hydrologic components using simplified procedures, including the unit hydrograph method, empirical formulas, and analytical equations. These so-called lumped parameter models do not consider spatially distributed processes.

[21] Moving from lumped parameter to distributed parameter approaches, numerical watershed models are now available that are based on multidimensional governing equations that allow for heterogeneous parameter distribution and heterogeneous boundary conditions. It is not yet clear whether these physically based distributed models are better predictors than lumped parameter models (see *Beven* [1989] and *Grayson et al.* [1992] for an extensive discussion). The application of physically based models to larger spatial scales is inherently problematic, because of the potential limitations of available model equations as applied to hetereogeneous hydrologic systems, the lack of a theory of subgrid-scale integration, and because of problems of dimensionality in parameter calibration [*Beven*, 1989]. These models usually employ, to various degrees, some form of lumping or spatiotemporal averaging over the local, plot, and field scale, thereby putting into question whether their parameters can be physically interpreted [*Feddes et al.*, 1993].

[22] Specifically, one may question the validity of Richards' equation to describe soil water flow at spatial scales representing field or watershed scales. It is our view, however, that like any other hydrologic model, flow models based on Richards' equation are applied as an approximation to the underlying hydrologic system to characterize the dynamics of spatially distributed drainage flow as a response to variable surface boundary conditions. Some may question whether Richards' equation is valid at all, even at the much smaller spatial scales of laboratory columns or small field plots often used to simulate flow and transport. Addressing this issue is beyond the scope of this paper.

[23] The presented approach takes the point of view that the modeling of large-scale vadose zone systems is hampered by a lack of accurate spatially distributed information on boundary conditions and hydrological measurements and parameters that would be required for a full physical application and interpretation of the governing physically based equation (1). Instead, it is proposed to use statistically based inverse modeling to estimate the probability distribution of "effective" hydrological parameters that pertain to the inherent large spatial and temporal scales of the hydrologic domain. The effective parameters are calibration parameters and their posterior (calibrated) distributions

reflect the uncertainties associated with model assumptions and boundary conditions.

[24] In this paper, we compare parameter uncertainty ranges and predictive capability of a physically based and a simplified bucket model. The models were applied to explicitly determine whether a physically based, distributed hydrologic modeling approach is preferable over the bucket model given the spatial and temporal scales of the data collected at BWD. Furthermore, two case studies are implemented with different spatial resolution of the model parameters. In case study I, spatially uniform parameters are estimated at the BWD scale. In case study II, inverse modeling is used to obtain spatially distributed parameter sets at the drainage unit scale, resulting in one parameter set for each of 24 drainage units.

2.2.1. Physically Based Soil Water Flow Modeling

[25] Equation (1) is solved numerically using a mass-lumped fully implicit finite difference method with adaptive time stepping. The dependence of K and h_m on θ is represented by van Genuchten-Mualem type models (see section 2.2.3). The nonlinearities arising from these functions are handled with Newton-Raphson linearization. The adapted numerical model used in this study is MODHMS [*Panday and Huyakorn*, 2004], an extension of the finite difference groundwater flow model MODFLOW [*McDonald and Harbaugh*, 1988]. The model constitutes a distributed fully coupled surface/vadose zone/groundwater flow model, based on state-of-the-art nonlinear computational algorithms and integrated with GIS-based graphical user interfaces.

[26] For the three-dimensional model, the spatial domain of the BWD was divided into 1536 200 × 200 m square cells, using approximately 16 grid cells per agricultural field (see Figure 2). In both the three-dimensional and the one-dimensional, vertical model, the soil profile was discretized into 14 layers using 10 top layers with a thickness of 0.30 m (1 foot) and four remaining layer thicknesses of 0.60 m (2 feet), 0.60 m, 0.9 m (3 feet), and 0.9 m, resulting in a total of 21,504 cells.

[27] The initial head distribution throughout the profile was estimated by assigning a drainage unit specific water content value, θ_{ini}, to the top nodal point of the finite difference grid, assuming hydrostatic equilibrium and a uniform soil. Subsurface drainage to the tile drains was simulated using a head-dependent function, with drain discharge proportional to the head above the drain and a drain conductance parameter:

$$\begin{array}{ll} Q = D_c[H - (Z_0 - D_d)] & H \geq Z_0 - D_d \\ Q = 0 & H < Z_0 - D_d \end{array} \tag{3}$$

where Q is the subsurface drainage (LT^{-1}), D_c is drain conductance (T^{-1}), H is total hydraulic head in the layer that contains the drain (L), Z_0 is land surface elevation (L), and D_d is drain depth (L). Since the exact drain depth, D_d, and drain conductance (D_c) for each drainage units were unknown, they were considered to be calibration parameters.

2.2.2. Boundary Conditions

[28] The fully integrated 3-D approach uses spatially distributed upper boundary conditions at field-scale resolution. The three-dimensional approach allows for lateral water flow through the unsaturated zone, for example, when fields are irrigated in sections, and also allows for continuously varying water table at the resolution of the finite difference grid (subfield scale). In case study I, the simulation domain of the three-dimensional model is the BWD, whereas in case study II, the simulation domain of the three-dimensional model is the drainage unit. The one-dimensional flow model was used to represent the water district scale (case study I) or the drainage unit scale (case study II) using appropriate upscaled boundary fluxes.

[29] We assumed that no flow occurred across the lateral and lower boundaries of each of the models. A previous study in Broadview Water District [*Vaughan et al.*, 1999] suggested that ignoring regional groundwater flows may lead to an underestimation of drainage flow. However, we found that most drainage units did not have drainage flows outside the growing season, indicating little or no regional groundwater contribution that may be considered as "base flow." In addition, detailed water balance computations of BWD and each drainage unit, as well as various preliminary model calibrations runs with different lower boundary conditions, including a head-dependent flux lower boundary condition, demonstrated that the flux across the bottom of the 6.0-m deep soil profile was negligible compared to the surface and drainage fluxes. For these calculations, total hydraulic head gradients were estimated using piezometric head observations from deep wells surrounding the BWD. Furthermore, a preliminary annual water balance of the entire district indicated that the magnitude of regional groundwater flows between the BWD and surroundings districts was small relative to the measurement accuracy of the other water balance components.

2.2.3. Soil Hydraulic Properties

[30] In order to solve equation (1), it is necessary to specify the water retention and unsaturated soil hydraulic conductivity function. These hydraulic relationships were defined by the van Genuchten-Mualem (VGM) parameters [*van Genuchten*, 1980; *Mualem*, 1976]:

$$S_e = \frac{\theta(h_\mathrm{m}) - \theta_\mathrm{r}}{\theta_\mathrm{s} - \theta_\mathrm{r}} = \begin{cases} [1 + (\alpha|h_\mathrm{m}|)^n]^{-m} & h_\mathrm{m} < 0 \\ 1 & h_\mathrm{m} \geq 0 \end{cases} \tag{4}$$

$$K(S_e) = \begin{cases} K_s S_e^l \left[1 - \left(1 - S_e^{1/m}\right)^m\right]^2 & h_\mathrm{m} < 0 \\ 1 & h_\mathrm{m} \geq 0 \end{cases} \tag{5}$$

where S_e (−) is the effective water saturation, θ_s and θ_r denote the saturated and residual water content ($\mathrm{L}^3\ \mathrm{L}^{-3}$), α (L^{-1}) and n (dimensionless) are curve shape parameters for the soil water retention curve, K_s denotes the saturated hydraulic conductivity, and l is a unitless fitting parameter for the unsaturated soil hydraulic conductivity function. In MODHMS, the parameter l is fixed at a value of 0.5. As outlined hereafter, rather than considering all VGM parameters as calibration parameters, spatially distributed soil hydraulic functions will be estimated using calibrated scaling factors.

2.2.4. Scaling of Soil Hydraulic Properties

[31] The scaling approach of *Miller and Miller* [1956] has been extensively used to characterize soil hydraulic spatial variability and to develop a standard methodology to assess the variability of soil hydraulic functions and their parameters [*Peck et al.*, 1977; *Hopmans and Stricker*, 1989; *Clausnitzer et al.*, 1992; *Tuli et al.*, 2001]. The single objective of scaling is to coalesce a set of hydraulic

Table 2. Values of the van Genuchten-Mualem Parameters for the Reference Soil Hydraulic Properties

Parameter	Value	Unit
θ_s	0.45	$cm^3\ cm^{-3}$
θ_r	0.10	$cm^3\ cm^{-3}$
α	0.02	cm^{-1}
n	1.25	–
K_s	14.82	$cm\ d^{-1}$

relationships into a single reference curve using scaling factors that describe the set as a whole. Using the scaling factors, the soil water retention and hydraulic conductivity curve of any drainage unit i can be related to the reference hydraulic functions $h_{m,ref}(\theta)$ and $K_{ref}(\theta)$ using

$$h_{m,i} = \frac{h_{m,ref}}{\chi_i} \tag{6}$$

$$K_i = \chi_i^2 K_{ref} \tag{7}$$

The hydraulic VGM parameters of the reference soil hydraulic functions for the BWD were estimated with the neural network model ROSETTA of *Schaap et al.* [1998] for a clay soil, which is the dominant soil type in the district (Natural Resources Conservation Service, Soil survey of western Fresno County, 2003, available at http://www.ca.nrcs.usda.gov/mlra02/). The ROSETTA computed values are listed in Table 2, and they represent effective soil hydraulic parameters throughout the 6.0-m profile. Although the physical basis for application of the scaling concept to scales of hundreds of meters and larger is not obvious, the scaling factor approach provides an effective means to describe spatial variability of soil hydraulic functions between drainage units, using a single parameter. In the absence of available data on the spatial distribution of soils within and between drainage units, and to limit the number of calibration parameters, we treated the soil in each drainage unit as homogeneous.

2.2.5. Preferential Transport to Tile Drains

[32] Water flow transport in the vadose zone as expressed by equation (1) does not describe the accelerated transport of water through preferential flow paths. Recent investigations by *Kohler et al.* [2001, 2003] demonstrated that preferential flow can be an important hydrologic component in agricultural field soils. A significant fraction of the infiltrated water may move through soil cracks and along roots, thereby short-circuiting the soil matrix pore space and reaching groundwater much faster than predicted from Richards' equation.

[33] Preferential flow in structured media is usually described using dual-porosity or dual-permeability models [*Šimůnek et al.*, 2003]. These types of models require a relatively large number of input parameters, and is not warranted because of the spatial and temporal resolution of the calibration data. For example, the dual-permeability model of *Gerke and van Genuchten* [1993] may require 16 parameters. To avoid problems of overparametrization, we initially considered a simpler, bimodal variant of the multimodal pore size distribution model developed by *Mohanty et al.* [1997], to account for potentially accelerated movement of water to a tile drain. This model simulates a rapid increase in the hydraulic conductivity near saturation by dividing the soil matrix into a capillary-dominated and a noncapillary-dominated flow domain. However, preliminary optimization runs for each of the drainage units in the BWD demonstrated that the parameters in the pore size distribution model of *Mohanty et al.* [1997] were not well determined by calibration to spatially distributed drainage data. At the spatial and timescales considered here, the simulation results were nearly identical to those obtained using a traditional solution of the Richards' equation with the unimodal VGM model (equations (1) with (4) and (5)). Hence we implemented the following lumped preferential flow mechanism in all considered models:

$$Q_{quick}(t) = f_b[P(t) + I(t)] \tag{8}$$

where Q_{quick} is the drainage by preferential flow (LT^{-1}), P denotes the weekly rainfall (LT^{-1}), I is the infiltrating irrigation water (LT^{-1}), and f_b is the fraction of applied water that bypasses the soil matrix (–), to be determined during model calibration. The corresponding water volume does not contribute to soil storage changes but moves directly in the tile drains. Similar approaches to simulate preferential water flow were presented by *Jarvis* [1994] and *Šimůnek et al.* [2003]. In this study, potential tail water generated by field runoff of applied irrigation water into the drain sumps is accounted for by the quick flow component as well. Thus the total subsurface discharge to the tile drains of each drainage unit was computed by adding the quick flow component to the drainage resulting from matrix flow into the groundwater. G. H. Schoups et al. (Multi-criteria optimization of a regional spatially-distributed subsurface water flow model, manuscript in preparation, 2004) will further elaborate on the validity of this model concept by comparing observed and model predicted drainage salinity concentrations.

2.2.6. Model Calibration and Evaluation

[34] We initially selected the following 5 calibration parameters: χ, D_c, D_d, f_b, and θ_{ini}. To increase flexibility in the retention function close to saturation we included θ_s as an additional calibration parameter. Moreover, since the model simulations were highly sensitive to the estimated ET_c, we included a crop ET correction parameter, f_c, as another calibration parameter, thereby allowing adjustment of computed actual transpiration rates to acknowledge the potential uncertainty associated with reported crop coefficients. For example, differences in values for crop coefficients as reported by *Snyder et al.* [1989] and *Allen et al.* [1998]) can be about 25%. Moreover, the calibrated effective crop coefficient values may effectively correct for water balance errors, caused for example by neglecting regional groundwater flow across the BWD and drainage unit boundaries. The final simulated actual ET_a was computed from the product of f_c and ET_c. These seven effective parameters make up the parameter set, Θ. The values of Θ were estimated by calibration using inverse modeling, against the spatially distributed, weekly drainage data that serve as calibration targets. The prior uncertainty ranges for each of these parameters are defined in Table 3, and apply to both the BWD and drainage unit scale. We note that the calibrated vadose zone model parameters, including the soil

Table 3. Calibration Parameters for the MODHMS Model, Including Their Prior Uncertainty Ranges

Parameter	Description	Minimum	Maximum	Unit
χ	scaling factor	0.01	10.0	-
D_c	drain conductance	0.00006	0.19	d^{-1}
D_d	drain depth	60.0	450.0	cm
θ_{ini}	initial water content	0.15	0.40	$cm^3\ cm^{-3}$
θ_s	saturated water content	0.25	0.50	$cm^3\ cm^{-3}$
f_c	crop coefficient adjustment factor	0.70	1.30	-
f_b	bypass fraction	0.00	0.30	-

hydraulic functions, represent effective soil properties, whose values can generally not be obtained by direct measurements [*Feddes et al.*, 1993].

[35] As is common in inverse modeling [*Hill*, 1998], we use the first part of the available data set (1995) for model calibration and the second half of the data set (1996) for model evaluation (validation). Such a split sample test provides the only means to test the validity of the calibrated parameters. To further examine the validity of the spatially distributed physically based hydrologic models we also evaluated the predictive capabilities of these models by comparing measured and simulated groundwater table depths at various locations within the BWD. As these spatially distributed water table depths were not used during the calibration, this is a much stronger test of the internal consistency of the model than the model validation based on measured drainage dynamics alone.

2.3. Storage-Based Bucket Model

[36] We compared the performance of the one- and three-dimensional MODHMS models with a simple bucket-type lumped storage-based model, BUCKET. For the bucket model, the vadose zone is conceptualized by two independent compartments in parallel, each characterized by the instantaneous water balance:

$$\frac{dS}{dt} = \text{in} - \text{out} \tag{9}$$

where S denotes soil water storage (L), "in" is the sum of all incoming fluxes (LT^{-1}), and "out" is the sum of all outgoing fluxes (LT^{-1}) using weekly time intervals. The first compartment represents the matrix flow domain, whereas the second compartment is the preferential flow domain. No interaction is allowed between the two compartments. The explicit forward-in-time finite difference approximation of the water balance equation for the matrix flow domain results in

$$S(t+\Delta t) = S(t) + \Delta t[(1-f_b)[P(t)+I(t)] - f_c ET_c(t) - E_s(t) - Q_{slow}(t)] \tag{10}$$

where Δt denotes the time step (T), and Q_{slow} is the slow (matrix) component of drainage (LT^{-1}). Drainage out of the matrix domain, Q_{slow}, was calculated as follows:

$$Q_{slow}(t) = \begin{cases} a\exp(b[S(t) - S_{min}]) & if \quad S(t) > S_{min} \\ 0 & if \quad S(t) \le S_{min} \end{cases} \tag{11}$$

where S_{min} (L) is the minimum storage needed to initiate drain flow from the matrix domain, a (LT^{-1}) denotes the minimum attainable drainage rate, and b (L^{-1}) is an additional fitting parameter describing the rate of drainage as a function of soil water storage. Equation (10) is solved for each time step starting from initial water storage, S_{ini}, using weekly time steps. Total drainage to the tile drain is computed according to

$$Q_{drain} = Q_{slow} + Q_{quick} \tag{12}$$

in which the quick flow component (Q_{quick}) is modeled the same way as in the physically based model. In conclusion, the bucket model contains six parameters, $S_{ini}, f_c, S_{min}, f_b$, a, and b. For each of the 25 drainage units, the prior ranges for each of these parameters are listed in Table 4.

2.4. Parameter Optimization by Inverse Modeling

[37] While much research has been devoted to developing automated procedures for calibration of lumped parameter models, automated parameter estimation for distributed physically based watershed models is a new area of research [*Madsen*, 2003]. Physically based distributed hydrologic models potentially contain a large number of model parameters which need to be estimated by calibration against a historical record of data. Specifically, for each of the drainage units within the BWD six or seven parameters need to be estimated, depending on which model is used. To improve parameter optimization methods, they need to be applicable for cases with large number of calibration parameters and must provide parameter uncertainties with corresponding model uncertainties. The SCEM-UA algorithm is a general purpose global optimization algorithm that provides an efficient estimate of the most likely parameter set and its underlying posterior probability distribution within a single optimization run.

[38] When using the SCEM-UA algorithm to retrieve the posterior distribution of the model parameters, the posterior density of each parameter set needs to be estimated. In this study, we used the following standard density function [*Box and Tiao*, 1973]:

$$p(\Theta|\boldsymbol{y}) \propto \left[\sum_{j=1}^{N} [\varepsilon_j(\Theta)]^2\right]^{-\frac{1}{2}N} \tag{13}$$

in which $p(\Theta|\boldsymbol{y})$ denotes the posterior density (assumed uniform a priori) given the parameter set Θ and observed data $\boldsymbol{y}$, and ε is a $N \times 1$ vector of residuals, which are calculated by computing the difference between the observed data $\boldsymbol{y}$ and the corresponding model predictions, $\hat{\mathbf{y}}$, of size N. In the remaining part of this paper, the stationary posterior distribution of the parameters is also referred to as the high probability density (HPD) region of

Table 4. Calibration Parameters of the Conceptual BUCKET Model, Including Their Prior Uncertainty Ranges

Parameter	Description	Minimum	Maximum	Unit
S_{ini}	initial storage	0.00	500.00	cm
S_{min}	minimum soil water storage	0.00	500.00	cm
a	minimum attainable drainage	0.00	10.0	$cm\ d^{-1}$
b	drainage parameter	0.00	1.00	cm^{-1}
f_c	crop coefficient adjustment factor	0.70	1.30	-
f_b	bypass fraction	0.00	0.30	-

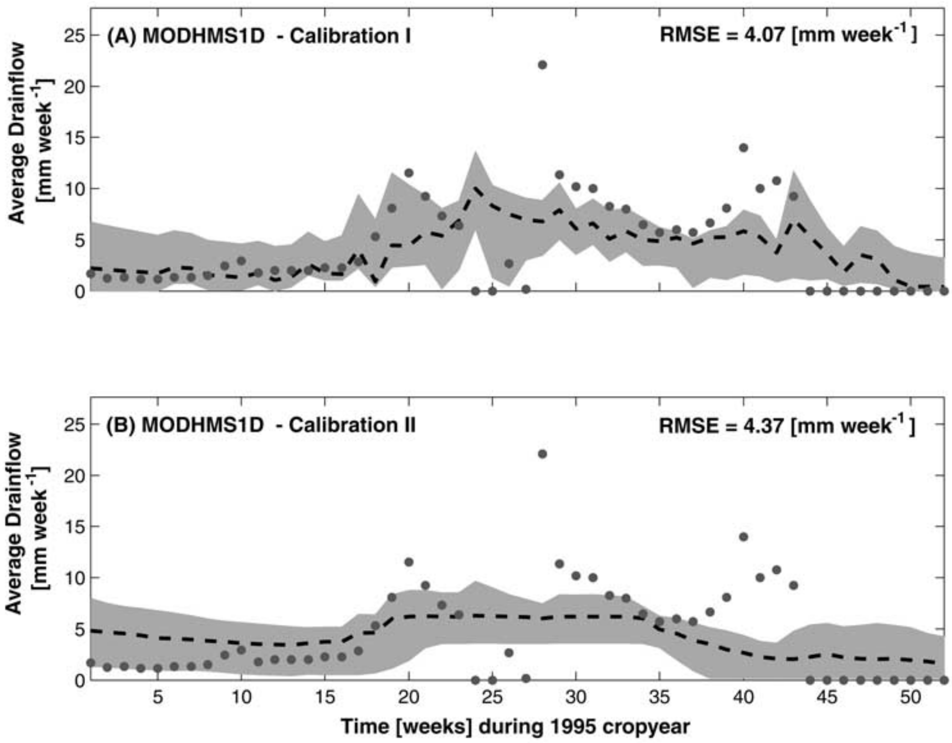

Figure 4. Influence of spatial and temporal discretization on performance of the MODHMS-1D model for drainage unit 4: (a) bi-daily boundary conditions in combination with 100 nodes in the vertical direction and (b) weekly boundary conditions and 14 nodes in the vertical direction. The dashed lines define the drainage rates for the most likely parameter set, whereas the gray shaded area in both plots denotes the MODHMS-1D prediction uncertainty ranges associated with the high probability density (HPD) region of the parameter space. The circles correspond to the drain flow observations.

the parameter space. The marginal parameter uncertainty ranges reported in the remainder of this paper correspond to the 0.5% and 99.5% percentiles of the stationarity posterior probability distribution.

[39] The posterior probability distribution for each of the optimization runs reported in this paper was estimated using 3000 trials with the SCEM-UA algorithm, resulting in an equal number of generated parameter sets and model runs. Convergence to a stationary posterior distribution was monitored by comparison of first- and second-order statistical moments for each of the parameters in the different SCEM-UA generated sequences. To reduce the computational time needed to perform each optimization run for the three-dimensional solution of the Richards' equation, the SCEM-UA algorithm was partly rewritten to facilitate parallel optimization using a prespecified number of computers. Specifically, in this study we used 10 Pentium IV 2.8 GHz computers to perform each of the 3000 MODHMS-3D model runs in parallel.

3. Results and Discussion

[40] In this section, we illustrate and discuss the results obtained when performing the various optimizations with the SCEM-UA algorithm. In particular, we explore the usefulness and applicability of the inverse method for the identification of soil and drainage system properties at the drainage unit and BWD district scale. Throughout this section we are especially concerned with the benefits of using a fully integrated three-dimensional solution of the Richards' equation (MODHMS-3D) by comparing its results with those obtained using the simplified conceptual bucket model (BUCKET) and the one-dimensional solution of the unsaturated flow equation (MODHMS-1D).

[41] To verify whether improved predictions of spatially distributed drainage data can be made by implementing finer spatial grid discretization and finer temporal discretization, we compared MODHMS-1D simulation results using bi-daily boundary conditions in combination with 100 nodes in the vertical direction (calibration I) with those using the weekly boundary conditions and 14 nodal values with depth (calibration II), as used in all subsequent modeling exercises. As an example, we present a comparison of drainage unit 4 in Figure 4. The two cases produce nearly identical RMSE values although the higher temporal discretizations produced improved temporal dynamics in the drainage discharge. In part, this is caused by outliers in the observations that cannot be simulated, irrespective of the discretization scheme.

3.1. Case Study I: Spatially Uniform (BUCKET and MODHMS-1D) and Spatially Distributed Boundary Conditions (MODHMS-3D) With Spatially Uniform Calibration Parameters

[42] The first case study investigates the ability of BUCKET and MODHMS-1D and -3D to predict spatially distributed drainage data based on district-wide uniform parameters. To accomplish the calibration for the one-

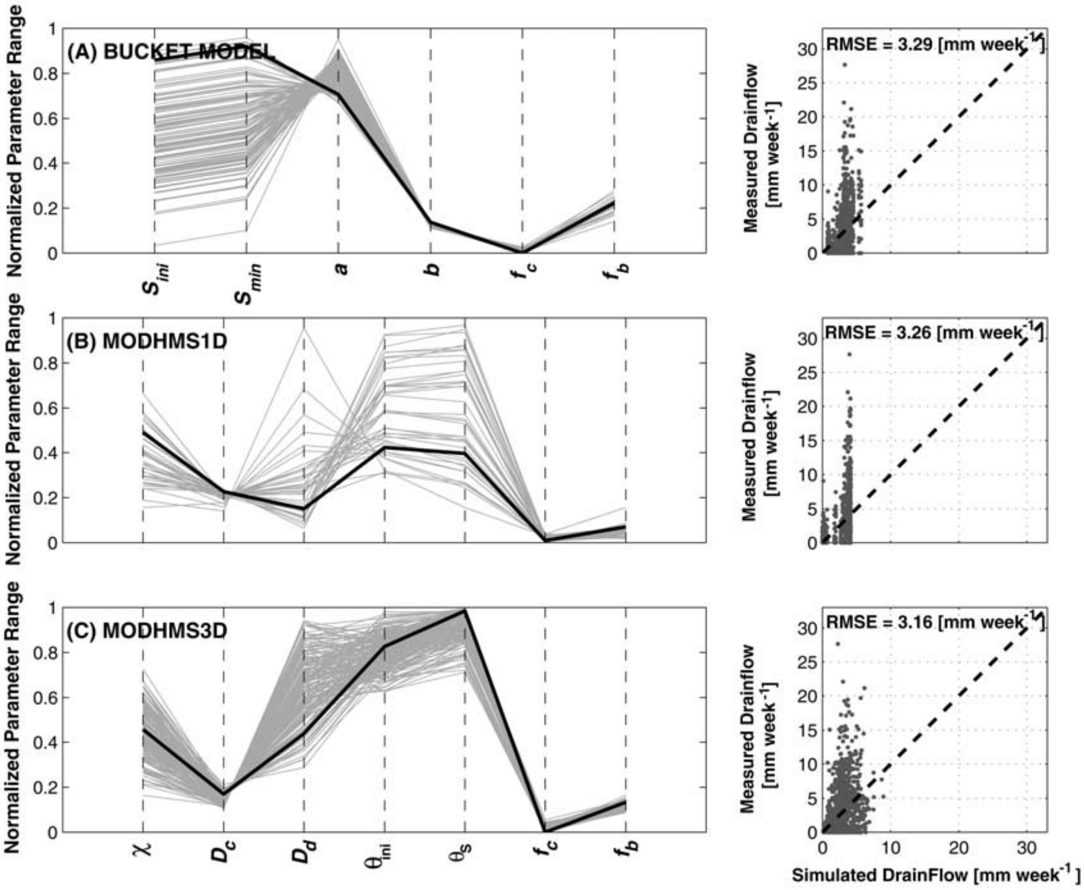

Figure 5. Case I: normalized uncertainly plots for each of the parameters of the (a) BUCKET, (b) MODHMS-1D, and (c) MODHMS-3D models, constructed using the results for the whole BWD calibration. The calibration parameters for each model are listed along the x axis, while the y axis corresponds to the parameter values, scaled according to their prior uncertainty ranges (defined in Tables 3 and 4) to yield normalized ranges between 0 and 1. Each gray line across the graph represents one member of the HPD region. The solid black line going from left to right across the plot corresponds to the mode of the posterior distribution. The scatterplots at the right-hand side depict simulated versus observed district-wide drainage data. The dashed lines represent the 1:1 line.

dimensional BUCKET and MODHMS-1D model, the district average boundary conditions were used (Figure 3), whereas the boundary conditions were spatially distributed across agricultural fields for the MODHMS-3D simulations. For each of the three models, the likelihood function of equation (13) included the discharge data of each of the 24 drainage units during the 1995 calibration year, resulting in a total of 1248 observations. The results of this calibration are summarized in Figures 5, 6 and 7.

[43] Figures 5a–5c present parameter plots for each of the members in the HPD region of the parameter space for the BUCKET, MODHMS-1D, and MODHMS-3D models, respectively. The parameters were scaled according to their prior uncertainty ranges defined in Tables 3 and 4 to yield normalized ranges. Additionally, Figure 5 (right) presents scatterplots of simulated versus observed drainage data. These scatterplots are created by plotting the model-predicted weekly average drainage values corresponding to the most likely parameter set against the corresponding observed values for each of the 24 different drainage units. The results of Figure 5 highlight several important observations. First, the parameters a, b, f_c, and f_b of the BUCKET model and the parameters D_c, and f_b of the MODHMS models are very well determined by calibration to spatially distributed drainage data, as shown by the narrow range of the HPD region in the prior physically plausible space for each of these parameters. Second, there is considerable uncertainty associated with the other parameters, regardless of the modeling approach. Particularly, the soil hydraulic parameters cannot be adequately characterized. Thus the scaling factor and saturated water content in the MODHMS-1D and -3D models are poorly defined, meaning that ''acceptable'' model simulations are found over a wide range of parameter values. It appears that much of the hydrologic regime of the BWD can be explained by a combination of drain system characteristics and preferential flow mechanisms.

[44] The scatterplots in Figure 5 show that the conceptual BUCKET and MODHMS-1D model do not capture the observed drainage discharge dynamics as well as the

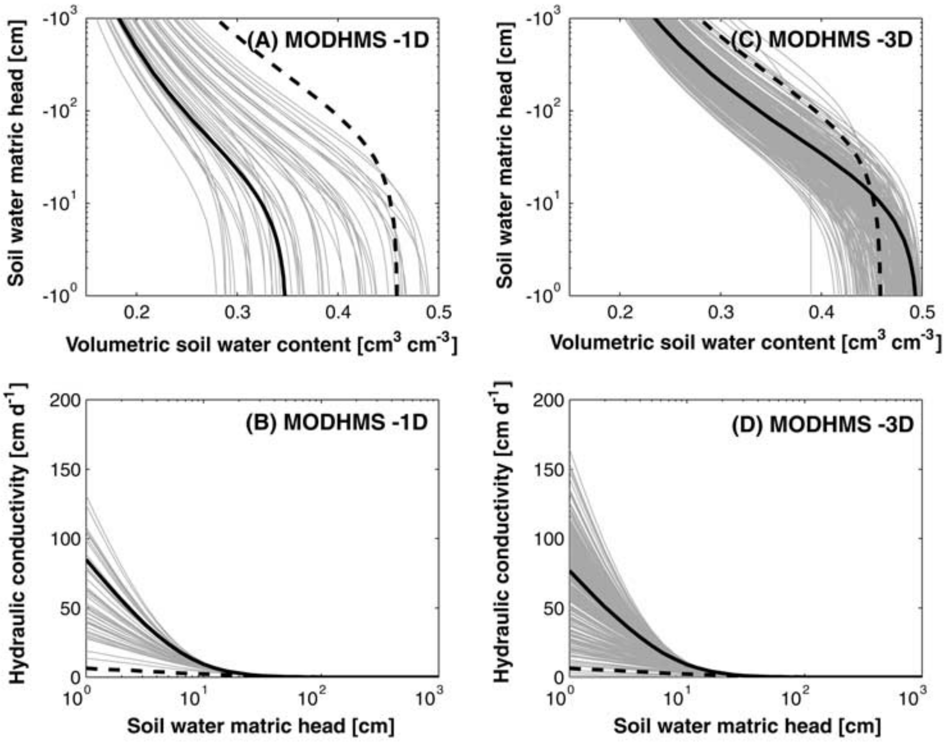

Figure 6. Case I: soil water retention and unsaturated soil hydraulic conductivity functions corresponding to each of the members of (a and b) MODHMS-1D in Figure 5 and (c and d) MODHMS-3D in Figure 5. The solid and dashed black lines correspond to the hydraulic functions of the most likely parameter set and reference curve, respectively.

MODHMS-3D model. The large variability in measured drainage flows within the BWD was primarily caused by the temporal variability in the start of irrigation events between different drainage units. Therefore, when distributing boundary conditions across fields in the MODHMS-3D simulations, the comparison improves slightly. Overall, all three models greatly underestimate drainflows at high discharge events, thereby causing some bias in the

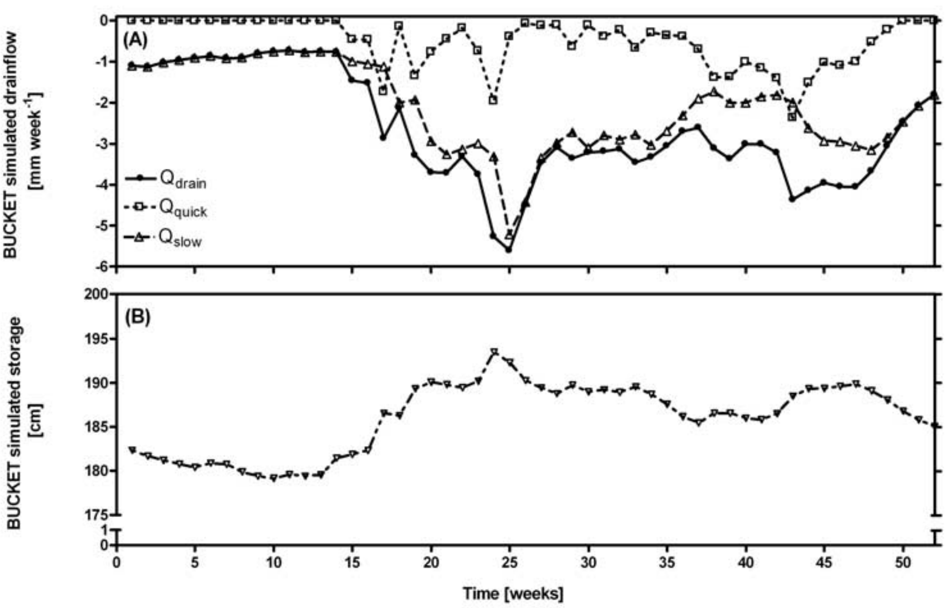

Figure 7. Case I: BUCKET model-simulated (a) slow flow, quick flow, and total drainage and (b) soil water storage over the 1995 calibration year, corresponding to the most likely identified parameter set.

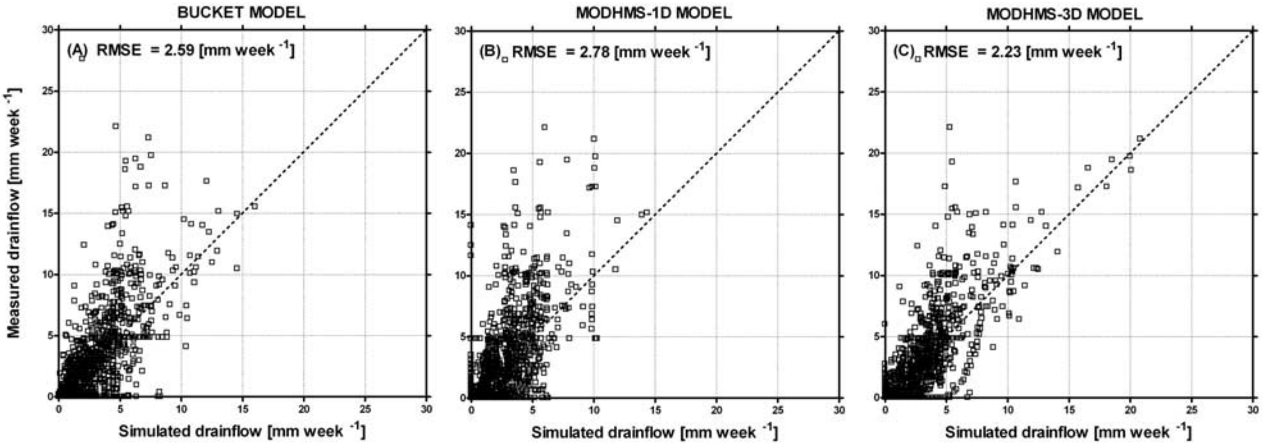

Figure 8. Case II calibration: scatterplot of simulated versus observed drain flow values for all drainage units, when assigning different parameter sets to each unit using the (a) BUCKET, (b) MODHMS-1D, and (c) MODHMS-3D models.

computed water balance. Note, however, that this bias is not due to neglected dynamical processes in the BUCKET and MODHMS models, but a natural consequence of the Bayesian density function implemented in this study. The classical calibration approach, which minimizes the squared residuals between model predictions and measurements, may give small RMSE values, but at the expense of considerable model bias [see *Boyle et al.*, 2000, Figure 5]. Parameter sets with minimal variance (lowest RMSE) tend to have a strong bias, whereas sets having close to zero bias have somewhat larger RMSE values.

[45] The inability of the inverse procedure to resolve a single, relatively unique set of hydraulic parameters from measured spatially distributed drainage data is further illustrated in Figure 6, which presents the soil water retention (Figures 6a and 6c) and unsaturated soil hydraulic conductivity functions (Figures 6b and 6d) for each of the members of the HPD region (Figures 5a and 5b). The significant uncertainty associated with the fitted soil water retention and unsaturated soil hydraulic conductivity functions, further supports the view that the soil hydraulic properties, at the spatial and temporal scales considered, are not well determined by calibration to measured drainage data. Consequently, when the hydrologic response is dominated by effective properties, such as drain depth, drain conductance and bypass flow, soil hydraulic properties may play only a minor role. We also note that the most optimal hydraulic properties, indicated with the black line, are well removed from the center of the prediction uncertainty bounds, suggesting a lognormal distribution of the scaling factor in the HPD region. Another significant and interesting observation is that the identifiability of the hydraulic parameters does not improve when increasing the spatial model dimension from 1 to 3. A similar conclusion was reported in previous work when comparing inversely estimated root water uptake parameters obtained with a one-, two-, and three-dimensional soil water flow model and spatially distributed soil water content data [*Vrugt et al.*, 2001].

[46] To assess the relative contributions of the quick and slow flow components to total simulated drainage, Figure 7a elucidates the BUCKET computed terms of the total drainage flow. For completeness, Figure 7b presents the corresponding BUCKET computed temporal changes in soil water storage, $S(t)$, from equation (10). Notice that the quick flow component is generally small compared to the slow flow component. Indeed, for each of the numerical models, the quick flow component (Q_{quick}) constitutes between 1

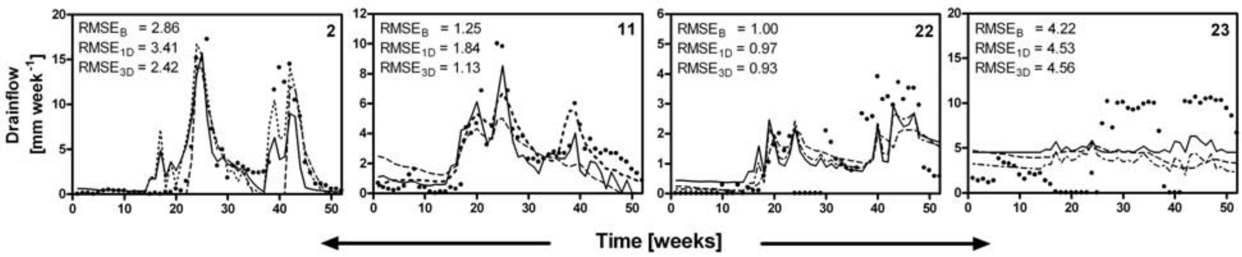

Figure 9. Case II calibration: drainage rates (mm week^{-1}) for a representative set of four drainage units (calibration case II) using the most likely parameter set for the BUCKET (solid line), MODHMS-1D (dashed line), and MODHMS-3D models (dotted line). Circles represent measured data.

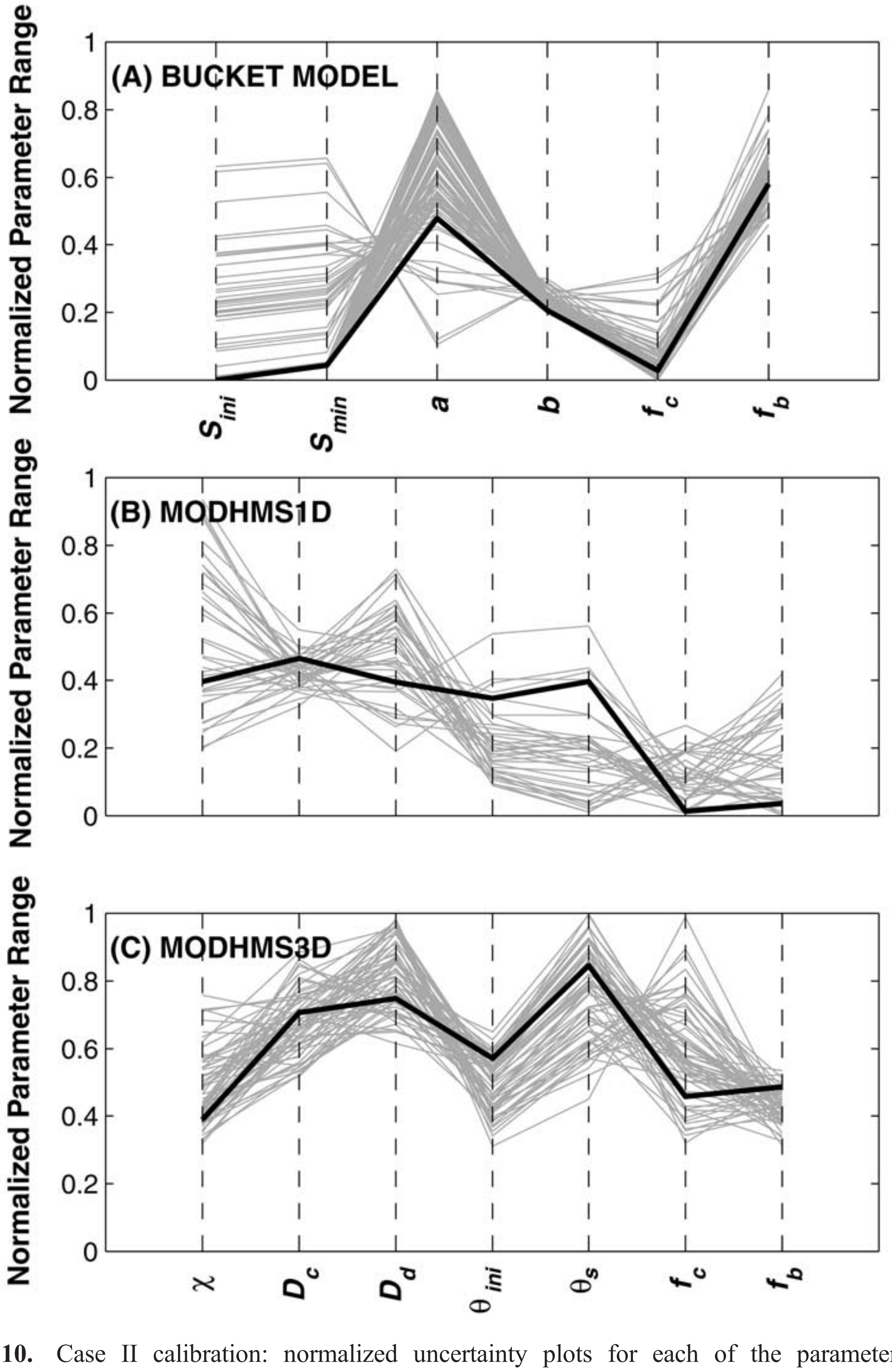

Figure 10. Case II calibration: normalized uncertainty plots for each of the parameters of the (a) BUCKET, (b) MODHMS-1D, and (c) MODHMS-3D models, constructed using the results for drainage unit 2. Each line across the graph denotes a single parameter set: The shaded lines are members of the HPD region; the solid line presents the most likely parameter set.

and 13% of the total simulated drainage flow (Q_{drain}) to the tile drains.

3.2. Case Study II: Spatially Distributed Boundary Conditions With Spatially Distributed Calibration Parameters

[47] In this case study we decreased the horizontal scale represented by the parameters, thereby increasing the number of estimated parameters. Individual parameters were estimated for each of the 24 drainage units, thereby distributing the parameters over the BWD. Preliminary optimization runs showed that water fluxes between adjacent drainage units were negligible (smaller than 5% of the total drainage unit drainage). Drainage units were, therefore, modeled individually. This approach is computationally not only more attractive, but also increases the prospects of finding the preferred parameter solutions for each of the drainage units, as only a limited

Table 5. Root-Mean-Square Error of the Drain Flow Predictions of Each of the Numerical Models for the Different Drainage Units of the BWD

	BUCKET		MODHMS-1D		MODHMS-3D	
Drainage Unit	Calibration	Validation	Calibration	Validation	Calibration	Validation
1	1.83	3.24	1.43	3.07	1.21	2.48
2	2.86	3.16	3.41	2.69	2.42	2.56
3	1.43	0.81	1.61	0.36	1.49	0.32
4	4.29	4.27	4.34	3.63	4.00	3.49
6	1.05	2.72	1.06	2.55	1.34	1.29
7	1.01	2.54	0.83	1.43	0.75	0.98
8	1.88	1.87	2.30	1.00	1.81	1.64
9	2.96	3.91	4.74	3.67	3.30	4.00
10	1.39	2.92	1.48	1.39	1.31	1.57
11	1.25	1.27	1.84	0.62	1.13	1.96
12	4.53	3.16	4.54	1.66	4.38	3.38
13	3.44	7.89	3.04	6.49	2.10	5.65
14	1.38	2.19	1.43	1.24	1.40	1.25
15	5.00	8.37	4.88	5.42	4.62	5.01
16	4.08	1.84	3.99	1.37	3.91	1.71
17	0.93	0.32	0.55	0.46	1.51	0.30
18	2.06	2.18	2.08	1.69	1.93	1.55
19	1.31	2.30	1.44	1.33	1.29	1.14
20	2.38	4.48	3.35	3.12	2.50	2.37
21	1.55	1.27	1.54	0.74	1.43	0.78
22	1.00	1.65	0.97	1.39	0.93	1.40
23	4.22	4.64	4.53	3.68	4.56	3.52
24	1.12	3.34	1.16	3.08	1.09	1.40
25	0.89	1.56	1.13	1.04	0.86	1.01

number of parameters need to be estimated in each optimization run. Hence, depending on whether the BUCKET or MODHMS models were used, 6 or 7 parameters were identified for each drainage unit by calibration to the weekly discharge data. The results are summarized in Figures 8, 9, and 10.

[48] Figures 8a–8c present scatterplots of simulated drainage flows, derived with the most likely parameter set, versus their observed values for the BUCKET, MODHMS-1D, and MODHMS-3D models, respectively, for the total set of drainage units. Compared to case study I, predictions of spatially distributed drainage data not only capture spatial patterns but perform much better in predicting temporal variations of individual drainage flows. In general, the MODHMS-3D model performs best and has the smallest RMSE. The larger RMSE of MODHMS-1D is the result of integrating boundary conditions (i.e., I and ET) to the entire drainage unit rather than modeling individual fields. At that reduced level of spatial resolution, the conceptual representation of the vadose zone by the BUCKET model exhibits fairly equal predictive capabilities. The benefits associated with the use of a three-dimensional physically based hydrologic model seem therefore relatively marginal, even when comparing the temporal dynamic behavior between the three models. However, the BUCKET model is computationally by far the most efficient, requiring less than 1 min to calibrate one drainage unit for 1 year of discharge data.

[49] To gain more insights into the performance of each model, Figure 9 presents the discharge simulation for a set of four representative drainage units (ranging from good to bad fit), using the most likely parameter set for the BUCKET (solid line), MODHMS-1D (dashed line), and MODHMS-3D (dotted line) model. The numbering used in the top right corner of each of the small plots in Figure 9 refers to the adopted numbering in Figure 2. Additionally, the top left corner of each plot presents summary statistics in terms of the RMSE of the residuals of the calibration period for each of the three models. Calibration summary statistics for all 24 drainage units, including those of Figure 9, are listed in Table 5. Results presented in Figure 9 and Table 5 show that the MODHMS-3D model has the most consistent predictions (lowest RMSE values). We note, however, that the fit to the observed drainage data for each of the models is fairly good for most drainage units, especially in the light of the measurement uncertainties associated with the surface boundary conditions and drainage data at these spatial scales.

[50] Since each drainage unit was treated as a separate simulation and parameter domain, we obtained 24 HDP plots similar to Figure 5, however, for illustrative purposes we only show the results of drainage unit 2 in Figure 10. However, similar results were found for the other drainage units. Disaggregation of the water district into individual drainage units does not reduce the amount of uncertainty associated with most of the parameters (compare Figure 5 with Figure 10) and in some cases even appears to increase parameter uncertainty. The results for each drainage unit, suggest that the only parameters that are well identifiable and, as such, are warranted by the spatially distributed drainage data are the parameters b and f_b of the BUCKET model, and the drain conductance, D_c, and bypass fraction, f_b, of the MODHMS models. The optimized values for the bypass flow parameter f_b for each of the different drainage units results in a contribution of quick flow to total drainage flow that ranges between 5 and 30%.

[51] Physical interpretation of the optimized hydraulic parameters of the MODHMS models is difficult since

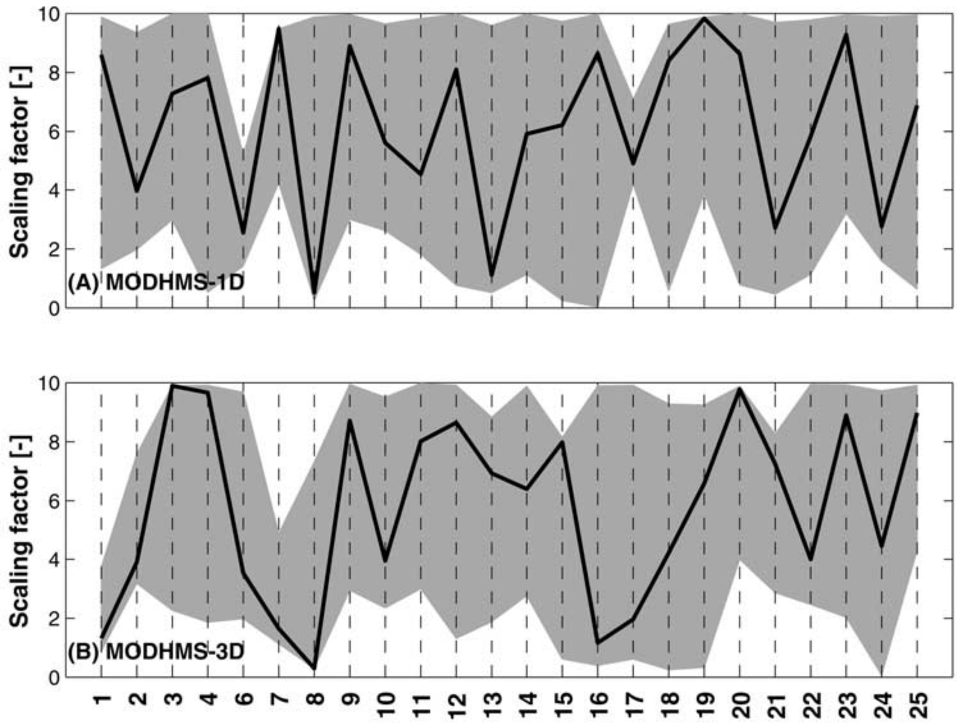

Figure 11. Case II calibration: SCEM-UA-derived parameter ranges of the HPD region of the scaling factor (y axis) for each of the different drainage units (listed along the x axis) in the (a) MODHMS-1D and (b) MODHMS-3D model. The solid line represents the most likely scaling factor for each of the drainage units.

these represent effective properties that are not only a function of soil type, but also depend on the boundary conditions [*Blöschl et al.*, 1995]. The large size of the HPD region of the scaling factor and saturated water content within the prior defined feasible parameter space and the resulting prediction uncertainty ranges of the soil water retention and unsaturated soil hydraulic conductivity functions, confirm our earlier conclusion that the effective soil hydraulic properties are poorly identifiable. To explore whether the nonidentifiability of the parameters in each of the models is caused by the poor quality of the models, the SCEM-UA derived parameter ranges for the scaling factors of both MODHMS values for all drainage units are presented in Figure 11. Regardless of the quality of the fit, the uncertainty associated with the scaling factor is considerable as for most drainage units the HPD region of the parameter space occupies almost the entire prior defined parameter range.

[52] Poorly constrained parameters may be caused by parameter correlation, poor model quality, and lack of parameter sensitivity as a result of insufficient information content [*Yapo et al.*, 1996]. For example, the latter could be the case if the spatially distributed drainage data do not contain the hydrologic conditions required to properly identify the soil hydraulic parameters. None of the parameter interactions in the MODHMS models were large enough to support parameter interaction as a major reason for poor identifiability of the soil hydraulic properties. This is illustrated in Table 6, which presents the generally small-valued correlation coefficients between the SCEM-UA generated parameter samples of the HPD region of the parameter space for both the MODHMS-1D and 3-D models. While the listed results correspond to drainage unit 2 only, similar correlation matrices were found for the other drainage units.

[53] Independent numerical optimizations using spatially distributed drainage data, generated from known parameter sets, confirmed that the measured spatially distributed drainage data contain only limited information content for the identification of the soil hydraulic properties. These results are not very surprising, as similar conclusions were drawn for the core-scale laboratory outflow experiments by *Toorman et al.* [1992] and *Eching and Hopmans* [1993]. From these studies it also became clear that additional measurements within the soil compartment are needed to improve the identifiability of the soil hydraulic parameters. We note that limited parameter identifiability is also caused by the potential uncertainties of the boundary conditions.

[54] To evaluate the consistency and reliability of the calibration results, the performance for each of the parameter sets in the HPD region for each of the three models was evaluated for the 1996 validation year. The most important results of this analysis are presented in Table 5 and in Figures 12, 13, and 14. Since most agricultural fields had different crops in 1996 (Table 1), the actual transpiration rates for the evaluation period were estimated by calibrating the crop coefficient adjustment factor, f_c, during 1996 using the SCEM-UA algorithm, while keeping the other calibration parameters equal to their most

Table 6. Correlation Coefficients Between the SCEM-UA–Generated Parameters in the HPD Region of the Parameter Space for Drainage Unit 2 Using the MODHMS-1D and MODHMS-3D Models[a]

	MODHMS-1D							MODHMS-3D						
	χ	D_c	D_d	θ_{ini}	θ_s	f_c	f_b	χ	D_c	D_d	θ_{ini}	θ_s	f_c	f_b
χ	**1.00**	0.47	0.46	0.46	**−0.50**	0.40	**0.51**	**1.00**	0.16	0.42	**0.52**	−0.24	0.12	−0.23
D_c	...	**1.00**	0.14	−0.17	0.07	0.46	0.34	...	**1.00**	0.30	0.29	0.46	0.07	0.29
D_d	...	...	**1.00**	−0.45	−0.27	0.25	0.05	...	...	**1.00**	**−0.56**	−0.42	0.48	0.03
θ_{ini}	...	...	...	**1.00**	**0.65**	−0.40	−0.48	...	...	...	**1.00**	**0.65**	**−0.53**	0.45
θ_s	...	...	...	...	**1.00**	−0.32	−0.41	...	...	...	...	**1.00**	**−0.54**	0.42
f_c	...	...	...	...	...	**1.00**	0.34	...	...	...	...	...	**1.00**	−0.12
f_b	...	...	...	...	...	...	**1.00**	...	...	...	...	...	...	**1.00**

[a]Boldface indicates an absolute value larger than 0.5.

probable values as estimated from the calibration. Adjusting the f_c parameter slightly (typically between 5 and 20%) improved the results. The drainage unit average initial water content profiles for 1996 were obtained using the simulated water content distribution of the most likely parameter set at the end of the year 1995.

[55] While the predictive capabilities of the conceptual and physically based models were similar for the 1995 calibration period, the 1996 validation results are slightly different, with the MODHMS-3D model consistently generating better forecasts (lowest RSME values) of measured drainage flow in most of the drainage units (Table 5 and Figures 12 and 13). The good quality fit of the MODHMS models to the measured 1996 drainage flows demonstrates that the information content of a single year is sufficient to obtain reliable estimates for most model parameters. In contrast, the performance of the BUCKET model is significantly less, when compared with the 1995 calibration period (Figures 8 and 9), suggesting that a longer calibration period may be needed to obtain reliable estimates of the model parameters. It therefore appears advantageous to use physically based hydrologic models at the temporal (week) and spatial (field) scales of this study.

[56] To further evaluate the predictive capability of the three calibrated models, we compared drainage unit average simulated groundwater table depths with their corresponding observed values (Figure 14). These latter values were obtained by arithmetically averaging groundwater table observations conducted within the same drainage unit. As these spatially distributed water table depths have not been used during calibration, their agreement is a much stronger test of the internal consistency of the calibrated model, than when evaluating the performance of the model on measured drainage dynamics only. While considerable scatter around the 1:1 line is apparent (RMSE values are 59.11 and 79.89 cm for the MODHMS-1D and MODHMS-3D model, respectively), there is no systematic bias: The arithmetic mean of predicted water table depths is reasonably close to the arithmetic mean of the measured water table depths, suggesting that the calibrated model is suited to predict the various components of the water balance at the scale of drainage units. The RMSE values are large but may be explained by significant spatial variability of water table elevations within fields, especially when field drains are present and fields are irrigated in sections.

4. Summary and Conclusions

[57] The aim of the present paper was to explore the usefulness and applicability of the inverse method to estimate vadose zone properties at the water district scale by using spatially distributed drainage data from the Broadview Water District located in the San Joaquin Valley of California. Results demonstrate that measured spatially distributed patterns of drainage flux data contain only limited information for the specification of the vadose zone model parameter calibration parameters, and are particularly inadequate for the soil hydraulic properties at those scales. In part, the inability of the

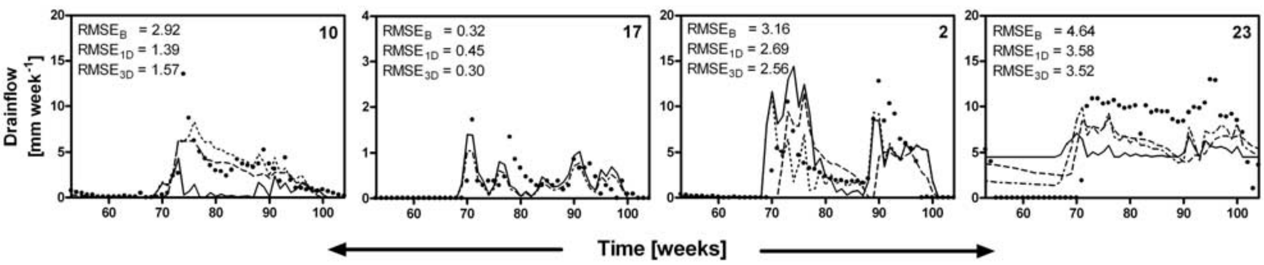

Figure 12. Case II validation: drainage rates (mm week^{-1}) for a selection of four representative drainage units using the most likely parameter set for the BUCKET (solid line), MODHMS-1D (dashed line), and MODHMS-3D models (dotted line). Circles represent measured data.

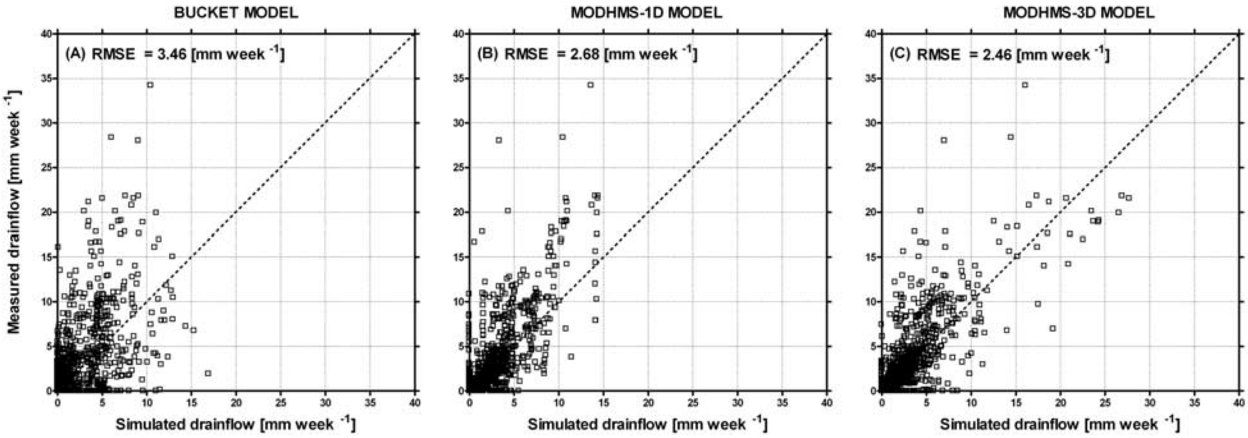

Figure 13. Case II-validation: Scatterplot of simulated versus observed drain flow values for all drainage units, when assigning different parameter sets to each unit using the (a) BUCKET, (b) MODHMS-1D, and (c) MODHMS-3D models.

inverse modeling approach to identify soil hydraulic properties at large spatial and temporal scales is a consequence of estimation errors in the boundary conditions and their uncertainty. The study showed that the only parameters with relatively small uncertainties are related to drain conductance and bypass flow. This result indicates that these are the critical parameters controlling the drainage flow processes at the considered space scale (field/drainage system) and timescale (week). Despite the large uncertainty of most calibration parameters, the fit to the observed drainage data for each of the models was fairly good for most drainage units. This is particularly true when considering the uncertainty in the drainage data and boundary conditions for these large time and space scales. We note especially that the predictive ability of the simple BUCKET model is about equal to that of the three-dimensional MODHMS model. Notwithstanding the significant CPU time needed for model calibration, there are advantages of using physically based hydrologic models to study spatial and temporal patterns of water flow at larger spatial scales. These mechanistic models not only generate consistent forecasts of spatially distributed drainage during both the calibration and validation periods but simultaneously possess unbiased predictive capabilities of groundwater table depths. In a later paper we will extensively discuss the various trade-offs in the fitting of drainage flow, drainage salinity, and groundwater table depths, by posing the optimization problem into a multicriteria framework and solving for the Pareto set of solutions using the recently developed Multiobjective Shuffled Complex Evolution Metropolis global optimization algorithm-University of Amsterdam/Arizona (MOSCEM-UA) of *Vrugt et al.* [2003c].

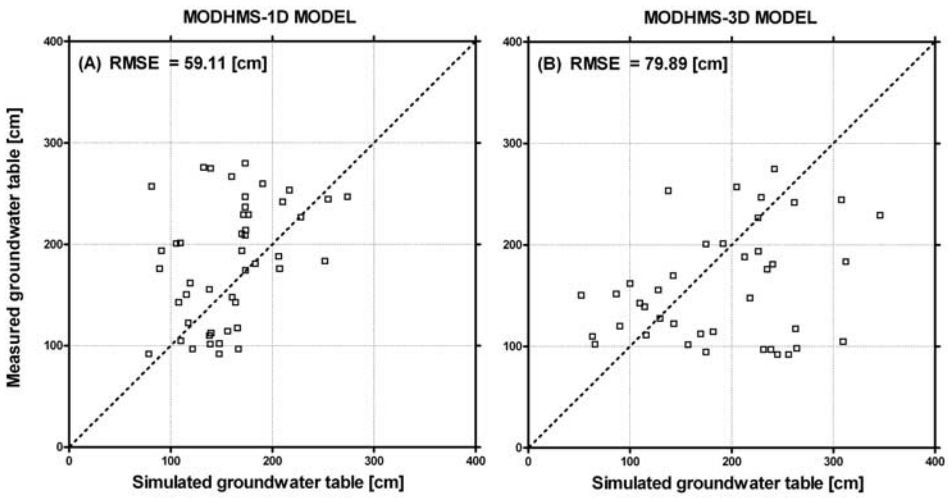

Figure 14. Case II cross validation: Scatterplot of drainage unit average simulated groundwater table depths versus observed values using the (a) MODHMS-1D and (b) MODHMS-3D models.

[58] **Acknowledgments.** The Earth Life Sciences and Research Council (ALW) supported the investigations of the first author with financial aid from the Netherlands Organization for Scientific Research (NWO). We acknowledge the support of HydroGeologic Inc. by providing us with a beta version of the MODHMS code. Some of the evaluation results would not have been possible without the cooperation of Peter Vaughan and Dennis Corwin by providing us with the groundwater data of the BWD. Computational support in the Department of LAWR was provided by Guido van Reenen, Bob Kehr, Ever Rivera, and Richard Massa. The current version of this paper has been greatly improved by constructive comments of three anonymous reviewers and the associate editor handling this manuscript.

References

Allen, R. G., L. S. Pereira, D. Raes, and M. Smith (1998), Crop evapotranspiration, guidelines for computing crop water requirements, in *FAO Irrigation and Drainage Paper 56*, report, pp. 135–158, Food and Agric. Organ., Rome.

Bates, B. C., and E. P. Campbell (2001), A Markov chain Monte Carlo scheme for parameter estimation and inference in conceptual rainfall-runoff modeling, *Water Resour. Res.*, *37*, 937–947.

Belitz, K. (1988), Character and evolution of the groundwater flow system in the central part of the western San Joaquin Valley, California, *U.S. Geol. Surv. Open File Rep.*, *87-573*, 34 pp.

Beven, K. (1989), Changing ideas in hydrology: The case of physically-based models, *J. Hydrol.*, *105*, 157–172.

Beven, K. (2001), How far can we go in distributed hydrological modeling, *Hydrol. Earth Syst. Sci.*, *5*, 1–12.

Blöschl, G., R. B. Grayson, and M. Sivapalan (1995), On the representative elementary area (REA) concept and its utility for distributed rainfall-runoff modeling, *Hydrol. Processes*, *9*, 313–330.

Bourgault, G., A. G. Journel, J. D. Rhoades, D. L. Corwin, and S. M. Lesch (1997), Geostatistical analysis of a soil salinity data set, *Adv. Agron.*, *58*, 241–292.

Box, G. E. P., and G. C. Tiao (1973), *Bayesian Inference in Statistical Analyses*, Addison-Wesley-Longman, Reading, Mass.

Boyle, D. P., H. V. Gupta, and S. Sorooshian (2000), Toward improved calibration of hydrologic models: Combining the strengths of manual and automatic methods, *Water Resour. Res.*, *36*, 3663–3674.

Ciollaro, G., and N. Romano (1995), Spatial variability of the soil hydraulic properties of a volcanic soil, *Geoderma*, *65*, 263–282.

Clausnitzer, V., J. W. Hopmans, and D. R. Nielsen (1992), Simultaneous scaling of soil water retention and hydraulic conductivity curves, *Water Resour. Res.*, *28*, 19–31.

Corwin, D. L., M. L. K. Carrillo, P. J. Vaughan, J. D. Rhoades, and D. G. Cone (1999), Evaluation of a GIS-linked model of salt loading to groundwater, *J. Environ. Qual.*, *28*, 471–480.

Duan, Q., V. K. Gupta, and S. Sorooshian (1992), Effective and efficient global optimization for conceptual rainfall-runoff models, *Water Resour. Res.*, *28*, 1015–1031.

Durner, W., E. B. Schultze, and T. Zurmühl (1997), State-of-the-art in inverse modeling of inflow/outflow experiments, in *Characterization and Measurement of the Hydraulic Properties of Unsaturated Porous Media*, *Proceedings of International Workshop, Riverside, CA. October 22–24*, edited by M. T. van Genuchten, F. J. Leij, and L. Wu, pp. 661–681, Univ. of Calif., Riverside.

Eching, S. O., and J. W. Hopmans (1993), Optimization of hydraulic functions from transient outflow and soil water pressure data, *Soil Sci. Soc. Am. J.*, *57*, 1167–1175.

Eching, S. O., J. W. Hopmans, and O. Wendroth (1994), Unsaturated hydraulic conductivity from transient multi-step outflow and soil water pressure data, *Soil Sci. Soc. Am. J.*, *58*, 687–695.

Feddes, R. A., P. J. Kowalik, and H. Zaradny (1978), *Simulation of Field Water Use and Crop Yield*, John Wiley, Hoboken, N. J.

Feddes, R. A., M. Menenti, P. Kabat, and W. G. M. Bastiaansen (1993), Is large-scale inverse modeling of unsaturated flow with areal average evaporation and surface soil moisture as estimated from remote sensing feasible?, *J. Hydrol.*, *143*, 125–152.

Gelhar, L. W. (1986), Stochastic subsurface hydrology from theory to applications, *Water. Resour. Res.*, *22*, 135S–145S.

Gerke, H. H., and M. T. van Genuchten (1993), A dual-porosity model for simulating the preferential movement of water and solutes in structured porous media, *Water. Resour. Res.*, *29*, 305–319.

Grayson, R., and G. Blöschl (2001), *Spatial Patterns in Catchment Hydrology*, 404 pp., Cambridge Univ. Press, New York.

Grayson, R., I. D. Moore, and T. A. McMahon (1992), Physically-based hydrologic modeling: 2. Is the concept realistic?, *Water Resour. Res.*, *28*, 2659–2666.

Harradine, F. (1950), Soil survey of western Fresno county, report, 86 pp., Univ. of Calif. Press, Berkeley, Calif.

Harter, T., and T. C. J. Yeh (1998), Flow in unsaturated random porous media, nonlinear numerical analysis and comparison to analytical stochastic models, *Adv. Water Resour.*, *22*, 257–272.

Harter, T., and D. Zhang (1999), Water flow and solute spreading in heterogeneous soils with spatially variable water content, *Water Resour. Res.*, *35*, 415–426.

Hill, M. (1998), Methods and guidelines for effective model calibration, *U.S. Geol. Surv. Water Resour. Invest. Rep.*, *98-4005*.

Hollenbeck, K. J., and K. H. Jensen (1998), Maximum-likelihood estimation of unsaturated soil hydraulic parameters, *J. Hydrol.*, *210*, 192–205.

Hopmans, J. W., and J. N. M. Stricker (1989), Stochastic analysis of soil water regime in a watershed, *J. Hydrol.*, *105*, 57–84.

Hopmans, J. W., J. Šimůnek, N. Romano, and W. Durner (2002a), Simultaneous determination of water transmission and retention properties—Inverse methods, in *Methods of Soil Analysis*: *Part 4, Physical Methods*, *SSSA Book Ser.* vol. 5, edited by J. H. Dane and G. C. Topp, pp. 963–1008, Soil Sci. Soc. of Am., Madison, Wis.

Hopmans, J. W., D. R. Nielsen, and K. L. Bristow (2002b), How useful are small-scale soil hydraulic property measurements for large-scale vadose zone modeling, in *Environmental Mechanics*: *Water, Mass and Energy Transfer in the Biosphere*, *Geophys. Monogr. Ser.*, vol. 129, edited by D. Smiles, P. A. C. Raats, and A. Warrick, pp. 247–258, AGU, Washington, D.C.

Jarvis, N. J. (1994), The MACRO Model (version 3.1): Technical description and sample simulations, *Rep. Diss. 19*, Dep. of Soil Sci., Swedish Univ. of Agric. Sci., Uppsala, Sweden.

Kohler, A., K. C. Abbaspour, M. Fritsch, M. T. van Genuchten, and R. Schulin (2001), Simulating unsaturated flow and transport in a macroporous soil to tile drains subject to an entrance head: Model development and preliminary evaluation, *J. Hydrol.*, *254*, 67–81.

Kohler, A., K. C. Abbaspour, M. Fritsch, and R. Schulin (2003), Using simple BUCKET models to analyze solute transport to subsurface drains by preferential flow, *Vadose Zone J.*, *2*, 68–75.

Kool, J. B., and J. C. Parker (1988), Analysis of the inverse problem for transient unsaturated flow, *Water Resour. Res.*, *24*, 817–830.

Kool, J. B., J. C. Parker, and M. T. van Genuchten (1985), Determining soil hydraulic properties for one-step outflow experiments by parameter estimation. I. Theory and numerical studies, *Soil Sci. Soc. Am. J.*, *49*, 1348–1354.

Kuczera, G., and E. Parent (1998), Monte Carlo assessment of parameter uncertainty in conceptual catchment models: The Metropolis algorithm, *J. Hydrol.*, *211*, 69–85.

Madsen, H. (2003), Parameter estimation in distributed hydrologic catchment modeling using automatic calibration with multiple objectives, *Adv. Water Res.*, *26*, 205–216.

McDonald, M. G., and A. W. Harbaugh (1988), A modular three-dimensional finite difference groundwater flow model, *U.S. Geol. Surv. Tech. Water Resour. Invest., Book 6, Chap. A1*, 588 pp.

Miller, E. E., and R. D. Miller (1956), Physical theory for capillary flow phenomena, *J. Appl. Phys.*, *27*(4), 324–332.

Mohanty, B. P., R. S. Bowman, J. M. H. Hendrickx, and M. T. van Genuchten (1997), New piecewise-continuous hydraulic functions for modeling preferential flow in an intermittent-flood-irrigated field, *Water Resour. Res.*, *33*, 2049–2063.

Mualem, Y. (1976), A new model for predicting the hydraulic conductivity of unsaturated porous media, *Water. Resour. Res.*, *12*, 513–522.

Panday, S., and P. S. Huyakorn (2004), A fully coupled physically-based spatially-distributed model for evaluating surface/subsurface flow, *Adv. Water Resour.*, *27*, 361–382.

Parker, J. C., J. B. Kool, and M. T. van Genuchten (1985), Determining soil hydraulic properties from one-step outflow experiments by parameter estimation. II. Experimental studies, *Soil Sci. Soc. Am. J.*, *49*, 1354–1359.

Peck, A. J., R. J. Luxmoore, and J. C. Stolzy (1977), Effects of spatial variability of soil hydraulic properties in water budget modeling, *Water Resour. Res.*, *13*, 348–354.

Romano, N., and A. Santini (1999), Determining soil hydraulic functions from evaporation experiments by a parameter estimation approach: Experimental verifications and numerical studies, *Water Resour. Res.*, *35*, 3343–3359.

Russo, D. (1988), Determining soil hydraulic properties by parameter estimation: On the selection of a model for the hydraulic properties, *Water Resour. Res.*, *24*, 453–459.

Santini, A., N. Romano, G. Ciollaro, and V. Comegna (1995), Evaluation of a laboratory inverse method for determining unsaturated hydraulic properties of a soil under different tillage practices, *Soil Sci.*, *160*, 340–351.

Schaap, M. G., F. J. Leij, and M. T. van Genuchten (1998), Neural network analysis for hierarchical prediction of soil water retention and saturated hydraulic conductivity, *Soil Sci. Soc. Am. J.*, *62*, 847–855.
Šimůnek, J., and M. T. van Genuchten (1996), Estimating unsaturated soil hydraulic properties from tension disc infiltrometer data by numerical inversion, *Water Resour. Res.*, *32*, 2683–2696.
Šimůnek, J., and M. T. van Genuchten (1997), Estimating unsaturated soil hydraulic properties from multiple tension disc infiltrometer data, *Soil Sci.*, *162*, 383–398.
Šimůnek, J., O. Wendroth, and M. T. van Genuchten (1998a), A parameter estimation analysis of the evaporation method for determining soil hydraulic properties, *Soil Sci. Soc. Am. J.*, *62*, 894–905.
Šimůnek, J., M. Šejna, and M. T. van Genuchten (1998b), HYDRUS-1D, version 2.0, software package and user documentation, 202 pp., Int. Ground Water Model. Cent., Colo. Sch. of Mines, Golden.
Šimůnek, J., N. J. Jarvis, M. T. van Genuchten, and A. Gärdenäs (2003), Review and comparison of models for describing nonequilibrium and preferential flow and transport in the vadose zone, *J. Hydrol.*, *272*, 14–35.
Snyder, R. L., B. J. Lanini, D. A. Shaw, and W. O. Pruitt (1989), Using reference evapotranspiration (ET_0) and crop coefficients to estimate crop evapotranspiration (ET_c) for agronomic crops, grasses, and vegetable crops, *Leaflet 21427*, pp. 1–12, Calif. Dep. of Water Resour., Sacramento, Calif.
Thyer, M., G. Kuczera, and Q. J. Wang (2002), Quantifying parameter uncertainty in stochastic models using the Box-Cox transformation, *J. Hydrol.*, *265*, 246–257.
Toorman, A. F., P. J. Wierenga, and R. G. Hills (1992), Parameter estimation of soil hydraulic properties from one-step outflow data, *Water Resour. Res.*, *28*, 3021–3028.
Tuli, A., K. Kosugi, and J. W. Hopmans (2001), Simultaneous scaling of soil water retention and unsaturated hydraulic conductivity functions assuming lognormal pore-size distribution, *Adv. Water Res.*, *24*, 677–688.
Valiantzas, J. D., and D. G. Kerkides (1990), A simple iterative method for the simultaneous determination of soil hydraulic properties from one-step outflow data, *Water Resour. Res.*, *26*, 143–152.
van Dam, J. C., J. N. M. Stricker, and P. Droogers (1992), Evaluation of the inverse method for determining soil hydraulic functions from one-step outflow experiments, *Soil Sci. Soc. Am. J.*, *56*, 1042–1050.
van Dam, J. C., J. N. M. Stricker, and P. Droogers (1994), Inverse method for determining soil hydraulic functions from multi-step outflow experiments, *Soil Sci. Soc. Am. J.*, *58*, 647–652.
van Dam, J. C., J. Huygen, J. G. Wesseling, R. A. Feddes, P. Kabat, R. E. V. van Walsum, P. Groenendijk, and C. A. van Diepen (1997), Theory of SWAP version 2.0, SC-DLO, *Rep. 71*, Dep. of Water Resour., Wageningen Agric. Univ., Wageningen, Netherlands.
van Genuchten, M. T. (1980), A closed form equation for predicting the hydraulic conductivity of unsaturated soils, *Soil Sci. Soc. Am. J.*, *44*, 892–898.
Vaughan, P. J., and D. L. Corwin (1994), A method of modeling vertical fluid flow and solute transport in a GIS context, *Geoderma*, *64*, 139–154.
Vaughan, P. J., S. M. Lesch, D. L. Corwin, and D. G. Cone (1995), Water content effect on soil salinity prediction: A geostatistical study using cokriging, *Soil Sci. Soc. Am. J.*, *59*, 1146–1156.
Vaughan, P. J., D. L. Suarez, J. Šimůnek, D. L. Corwin, and J. D. Rhoades (1999), Role of groundwater flow in tile drain discharge, *J. Environ. Qual.*, *28*, 403–410.
Vrugt, J. A., and W. Bouten (2002), Validity of first order approximations to describe parameter uncertainty in soil hydrologic models, *Soil Sci. Soc. Am. J.*, *66*, 1740–1751.
Vrugt, J. A., M. T. van Wijk, J. W. Hopmans, and J. Šimůnek (2001), One, two, and three-dimensional root water uptake functions for transient modeling, *Water Resour. Res.*, *37*, 2457–2470.
Vrugt, J. A., W. Bouten, H. V. Gupta, and J. W. Hopmans (2003a), Toward improved identifiability of soil hydraulic parameters: On the selection of a suitable parametric model, *Vadose Zone J.*, *2*, 98–113.
Vrugt, J. A., H. V. Gupta, W. Bouten, and S. Sorooshian (2003b), A Shuffled Complex Evolution Metropolis algorithm for optimization and uncertainty assessment of hydrological model parameters, *Water. Resour. Res.*, *39*(8), 1201, doi:10.1029/2002WR001642.
Vrugt, J. A., H. V. Gupta, L. A. Bastidas, W. Bouten, and S. Sorooshian (2003c), Effective and efficient algorithm for multiobjective optimization of hydrologic models, *Water Resour. Res.*, *39*(8), 1214, doi:10.1029/2002WR001746.
Vrugt, J. A., H. V. Gupta, S. Sorooshian, T. Wagener, and W. Bouten (2004), Confronting parameter uncertainty in hydrologic modeling: Application of the SCEM-UA algorithm to the Sacramento Soil Moisture Accounting Model, *J. Hydrol.*, in press.
Wildenschild, D., J. W. Hopmans, C. M. P. Vaz, and M. L. Rivers (2001), Using x-ray beams to study flow processes in underground porous media, *Adv. Photon Source Res.*, *4*, 48–50.
Yapo, P. O., H. V. Gupta, and S. Sorooshian (1996), Automatic calibration of conceptual rainfall-runoff models: Sensitivity to calibration data, *J. Hydrol.*, *181*, 23–48.
Zachmann, D. W., P. C. Duchateau, and A. Klute (1981), The calibration of Richards flow equation for a draining column by parameter identification, *Soil. Sci. Soc. Am. J.*, *45*, 1012–1015.
Zachmann, D. W., P. C. Duchateau, and A. Klute (1982), Simultaneous approximation of water capacity and soil hydraulic conductivity by parameter identification, *Soil. Sci.*, *134*, 157–163.
Zhang, D. (2002), *Stochastic Methods for Flow in Porous Media: Coping With Uncertainties*, Academic, San Diego, Calif.
Zurmühl, T., and W. Durner (1998), Determination of parameters for bimodal hydraulic functions by inverse modeling, *Soil Sci. Soc. Am. J.*, *62*, 874–880.

W. Bouten and J. A. Vrugt, Universiteit van Amsterdam, Institute for Biodiversity and Ecosystem Dynamics, Faculty of Science, Nieuwe Achtergracht 166, 1018 WV Amsterdam, Netherlands.

T. Harter, J. W. Hopmans, G. Schoups, C. Young, and W. W. Wallender, Hydrology Program, Department of Land, Air and Water Resources, University of California, Davis, Davis, CA, USA. (jwhopmans@ucdavis.edu)